Design, Synthesis and Biological Characterization of Histone Deacetylase 8 (HDAC8) Proteolysis Targeting Chimeras (PROTACs) with Anti-Neuroblastoma Activity

Salma Darwish[1,2], Ehab Ghazy [1, 2], Tino Heimburg[1], Daniel Herp[3], Patrik Zeyen[1], Rabia Salem-Altintas[4,5,6], Johannes Ridinger[4,5,6], Dina Robaa[1], Karin Schmidtkunz[3], Frank Erdmann[1], Matthias Schmidt[1], Chris Romier[7], Manfred Jung[3], Ina Oehme[4,5,6], Wolfgang Sippl[1*]

[1] Department of Medicinal Chemistry, Institute of Pharmacy, Martin-Luther University of Halle-Wittenberg, 06120 Halle/Saale, Germany

[2] Department of Pharmaceutical Chemistry, Faculty of Pharmacy, Alexandria University, 21521 Alexandria, Egypt

[3] Institute of Pharmaceutical Sciences, University of Freiburg, 79104 Freiburg, Germany

[4] Hopp Children's Cancer Center Heidelberg (KiTZ), Im Neuenheimer Feld 280, 69120 Heidelberg, Germany

[5] Clinical Cooperation Unit Pediatric Oncology, German Cancer Research Center (DKFZ), Im Neuenheimer Feld 280, 69120 Heidelberg, Germany

[6] German Cancer Consortium (DKTK), Im Neuenheimer Feld 280, 69120 Heidelberg, Germany

[7] Université de Strasbourg, CNRS, INSERM, Institut de Génétique et de Biologie Moléculaire et Cellulaire (IGBMC), Département de Biologie Structurale Intégrative, 67404 Illkirch Cedex, France

*corresponding author email : wolfgang.sippl@pharmazie.uni-halle.de

Abstract

In addition to involvement in epigenetic gene regulation, histone deacetylases (HDACs) regulate multiple cellular processes through mediating the activity of non-histone protein substrates. The knockdown of HDAC8 isozyme is associated with the inhibition of cell proliferation and apoptosis enhancement in several cancer cell lines. As previously shown, HDAC8 can be considered a potential target in the treatment of cancer forms such as childhood neuroblastoma. The present work describes the development of proteolysis targeting chimera (PROTAC) of HDAC8 based on substituted benzhydroxamic acids previously reported as potent and selective HDAC8 inhibitors. Within this study, we investigated the HDAC8-degrading profiles of the synthesized PROTACs and their effect on the proliferation of neuroblastoma cells. The combination of chemical synthesis, *in vitro* screening and cellular testing resulted in selective HDAC8 PROTACs that show anti-neuroblastoma activity in cells.

Keywords: histone deacetylases (HDAC), HDAC8, proteolysis targeting chimera (PROTAC), neuroblastoma, synthesis

I. Introduction:

Reversible acetylation and acylation of histone tails influence gene expression. While acetylation is catalysed by histone acetyltransferases (HAT), the removal of the acetyl mark is catalysed by histone deacetylases (HDACs). Besides histones these opposing enzymes regulate many cellular processes through dynamic acetylation and deacetylation of non-histone proteins such as transcription factors (p53), nuclear import factors and cytoskeletal proteins (α-tubulin). Abnormal acetylation/acylation of histones and non-histone proteins has been found to contribute to the development of various diseases [1-3]

Neuroblastoma is the most common childhood extracranial solid tumour. It emerges from precursor cells in the sympathetic nervous system leading to the development of tumours in the adrenal glands and/or the sympathetic ganglia. [4].

HDAC8 is a unique class I zinc-dependant HDAC. From all classical HDACs only HDAC8 overexpression was significantly correlated with the advanced stage of the disease and metastasis. Furthermore, it was found to be downregulated in 4S neuroblastoma cases. From the different patient groups, the 4S group, is characterised by increased spontaneous incidence of regression and high survival rate despite metastasis into liver, skin and bone marrow. Also, inhibition of proliferation, and induction of cell cycle arrest and differentiation such as the outgrowth of neurite-like structures was achieved in cultured neuroblastoma cells by the knockdown of HDAC8 [5,6]. Consequently, selective HDAC8 inhibition or degradation is a promising therapeutic strategy in neuroblastoma.
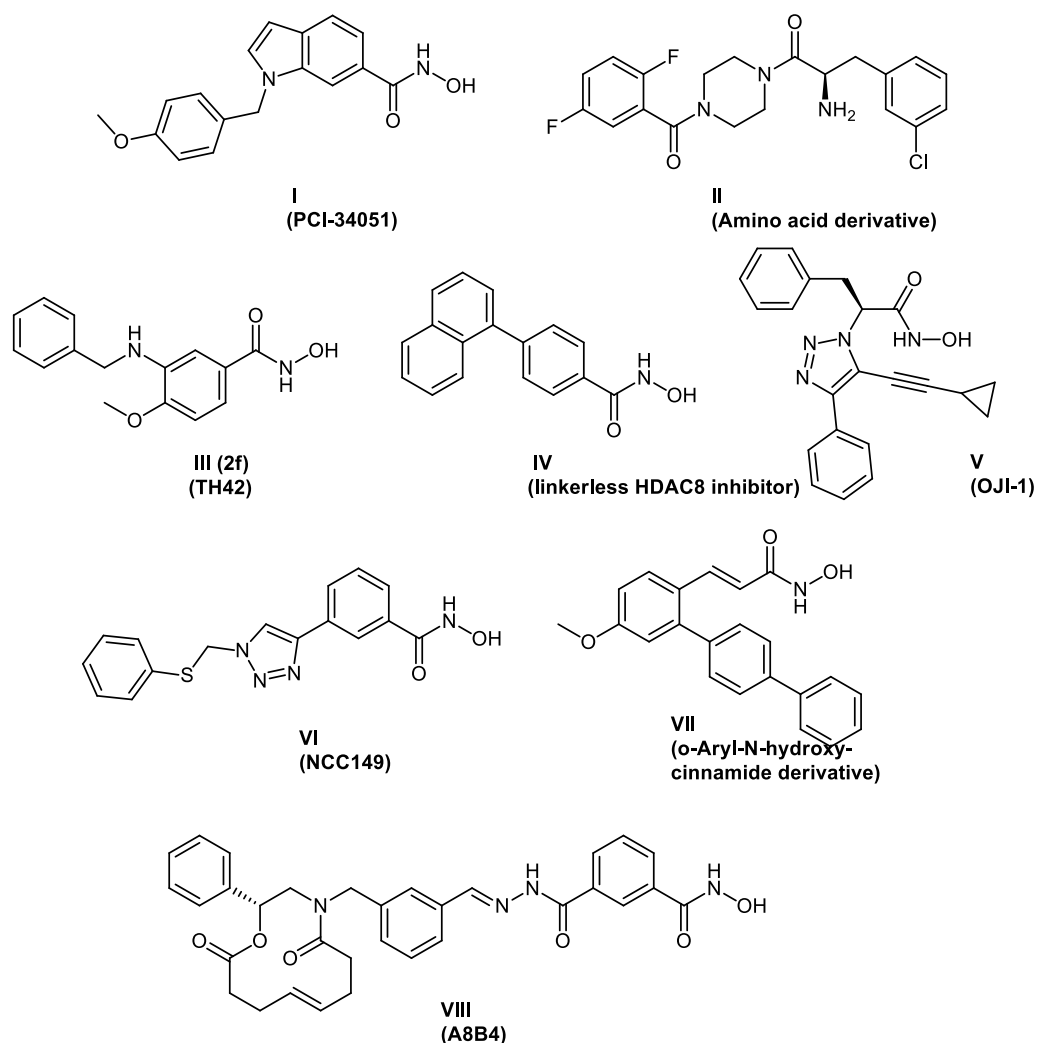
Figure 1. Chemical structures of reported HDAC8 inhibitors.

In recent years, several HDAC8 inhibitors have been reported (representative examples in Fig. 1.) [7-16]. In 2008, PCI-34051 **I** was reported as a potent and selective HDAC8 inhibitor. It shows good selectivity *in vitro* for HDAC8 compared to other subtypes tested (HDACs 1, 2, 3, 6 and 10) [7].

Chemotypes other than hydroxamic acids have also been reported to potently inhibit HDAC8. In the investigation made by Whitehead et al., the amino acid derivative **II**

showed good activity against HDAC8 (IC_{50} of 0.20 µM) accompanied with a good selectivity profile against HDAC1, HDAC2 and HDAC6 [15].

In 2017, we reported the synthesis of a series of para-substituted 3-aminobenzhydroxamic acids as potent HDAC8 inhibitors. Compound **III** with a methoxy group in the para position exhibited strong HDAC8 inhibitory activity (IC_{50} = 0.07 µM) coupled with selectivity over both HDAC isoforms 1 and 6. In addition, compound **III** showed anti-proliferative effect in several neuroblastoma cell lines [16].

The aforementioned HDAC8 inhibitors were designed based on the occupancy pharmacology in which the inhibitor exerts its function only by occupying a well-defined active or allosteric site instead of the biological substrate. The developed small molecules have to bind to the targeted site with strong affinity. This approach is connected with the evolution of side effects and resistance [17]. On the other hand, targeted protein degradation aims to induce degradation of the targeted protein specifically through hi-jacking the cellular protein quality control machinery. It offers a new concept to chemically knock-out protein targets and in recently reported studies several advantages over the classical occupancy-driven approach have been discussed in details [17-19].

Proteolysis targeting chimeras (PROTACs) are heterobifunctional molecules composed of a protein targeting warhead and an E3 ligase ligand linked by a linker. That way it can bind the protein targeted for degradation and the E3 ligase simultaneously. The key of success in developing the bifunctional molecule is the right pairing of an E3 ligase recruiting ligand with a POI targeting ligand and linking both with a suitable linker. When the linker employed possesses the appropriate flexibility and length, ubiquitination of the protein of interest can take place. The

labelled protein is recognized by the 26S proteasome and degraded [20,21]. Several types of PROTACs are available based on the different properties and characteristics of the E3-ligase ligands [22-26] and the POI warheads [27-30].

In 2019, the orally bioavailable bifunctional molecules ARV-110 and ARV471 (**Fig. 2**) were the first PROTACs to enter human clinical trials. While ARV-110 targets androgen receptors and is aimed to treat prostate cancer [31], ARV-471 targets estrogen receptor alpha and should be used in treatment of breast cancer [32]. As a result of their promising results and their acceptable safety and tolerability, these two PROTACs are currently in phase 2 trials [33]. These examples prove that PROTAC technology is a promising therapeutic approach.

Another approach to protein degradation is based on the attachment of hydrophobic labels to the desired inhibitors. Taking the knowledge that in eukaryotic cells, exposed hydrophobic residues in misfolded proteins result in their degradation, Neklesa et al. and Long et al. proved that covalent [34,35] and non-covalent [36] attachment of hydrophobic groups to the POI, target it for degradation by the cell's quality control machinery. The most studied and applied hydrophobic markers are adamantyl group [34,35] and tert-butyl carbamate-protected arginine (Boc3Arg) moieties [36]. Similar to a PROTAC, the bifunctional molecule employed for hydrophobic tagging (HyT) is composed of a hydrophobic group, a ligand of the POI linked together through a linker [17,34,37].

The hydrophobic label can initiate the proteasomal degradation either through destabilizing the POI [17,34,38], thereby recruiting chaperones to it or getting directly recognized by the chaperones [17,39]. In both cases the chaperones mediate the

proteasomal degradation. The latter can take place in different ways that are discussed in details in several references [34,36,38-40].

During the past decade some examples of degraders utilizing the hydrophobic tagging strategy have been developed. One of these is the first-in-class enhancer of zeste homolog 2 (EZH2) selective degrader MS1943 (**Fig. 2**) [41]. TX2-121-1 (**Fig. 2**) is another bifunctional degrader which leads to partial degradation of Her3 and reduction of Her3-dependant signalling [42]. More examples are discussed in the following references [43-45].
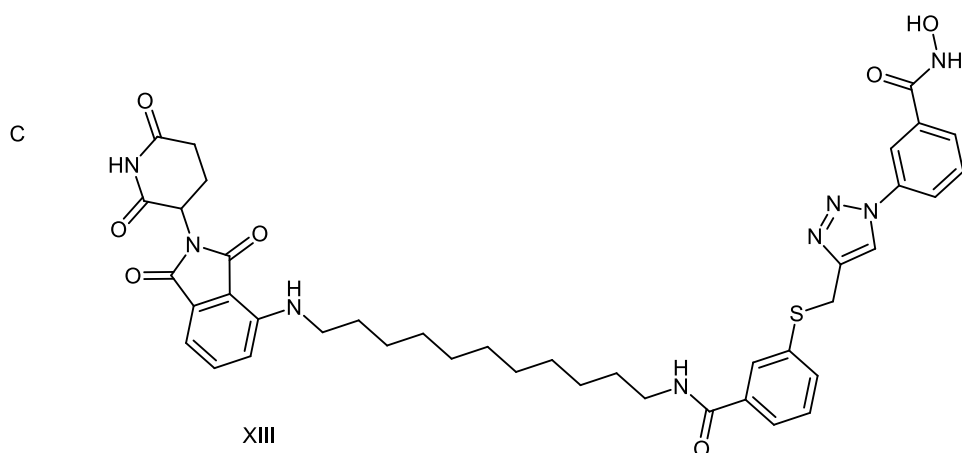
A

IX (ARV-110)

X (ARV-471)

B

XI (MS1943)

XII (TX2-121-1)

C

XIII
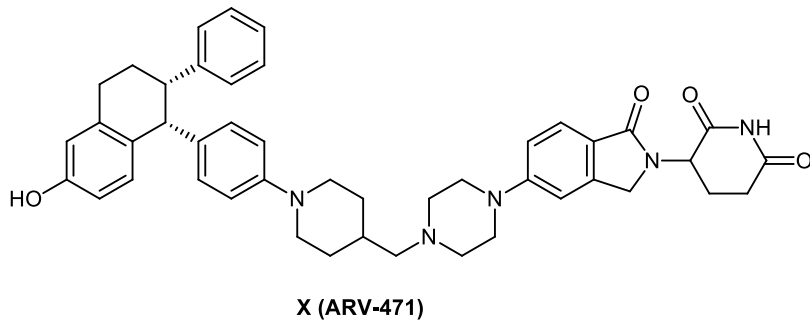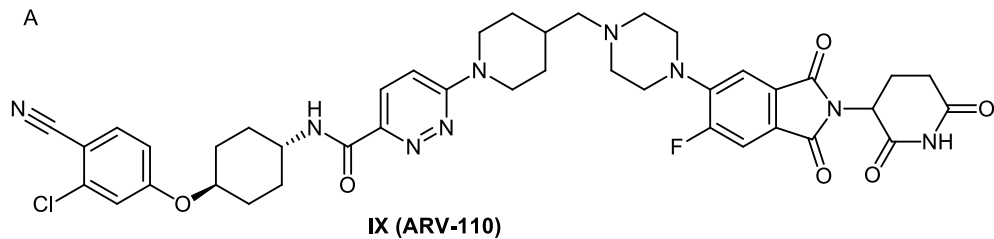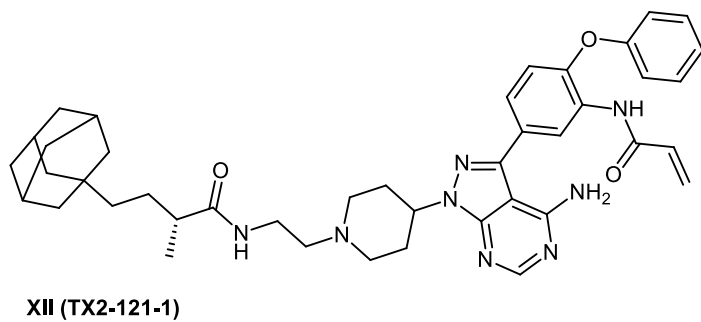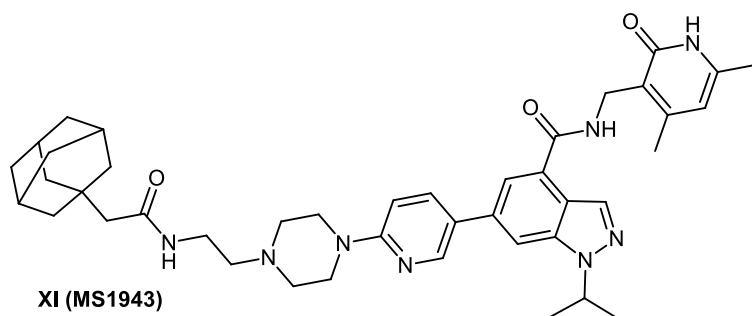
Figure 2. A) First PROTACs to enter in-human clinical trials. **B)** Examples of reported bifunctional hydrophobically tagged molecules. **C)** Reported HDAC8 PROTAC.

In the past few years, increasing interest to target HDACs using the PROTAC technology developed. In 2018, we published the development of the first degrader of an epigenetic eraser protein which was the Sirt2 deacetylase [28]. In the same year, Yang et al. were able to synthesize the first HDAC6 PROTAC utilizing a non-selective HDAC-inhibitor. [46]. After the development of this degrader, several PROTACs targeting HDAC6 enzyme were developed [47-49]. Also a first-in-class HDAC3 specific PROTAC was reported [50].

Recently Chotitumnavee et al. [51] reported the development of a HDAC8 PROTAC. In the three presented degraders the reported NCC-149 analouge [10] was taken as POI ligand and pomalidomide as E3 ubiqutin ligase ligand. Both warheads were connected with aliphatic linkers of three different lengths. From the synthesized degraders compound **XIII** (**Fig. 2**) resulted in efficient degradation of HDAC8 enzyme in T-cell leukemia Jurkat cells without affecting the levels of HDACs 1, 2 and 6.

In the present work we aimed at the development of bifunctional molecules that potently and selectively degrade HDAC8 in neuroblastoma cells, while not affecting the activity of the other HDAC isozymes. A further focus was the analysis of the antiproliferative effects of the PROTACs in neuroblastoma cell lines.

II.   Results and Discussion

The developed degraders (**1a-p, Table 1B**) were built based on previously published HDAC8 inhibitors possessing IC_{50} values in the low nanomolar range [52,16] (**Table 1A**). In previous studies, we found that benzhydroxamates showed good hHDAC8 inhibitory activity and selectivity over hHDAC1 and 6. Crystallographic studies as well as molecular docking studies on several HDAC subgtypes [53] revealed that the selectivity of this series of compounds can be attributed to the fact that the aromatic capping group occupies an HDAC8-specific pocket, which is absent in the other HDAC isoforms. Based on these findings, and the fact that the aromatic capping group of the HDAC inhibitors is facing towards the exit of the binding tunnel it can be used as an attachment point for a linker. The *p*-position of the phenyl capping group was chosen as an appropriate point for the attachment of the linker (**Figure 3**).
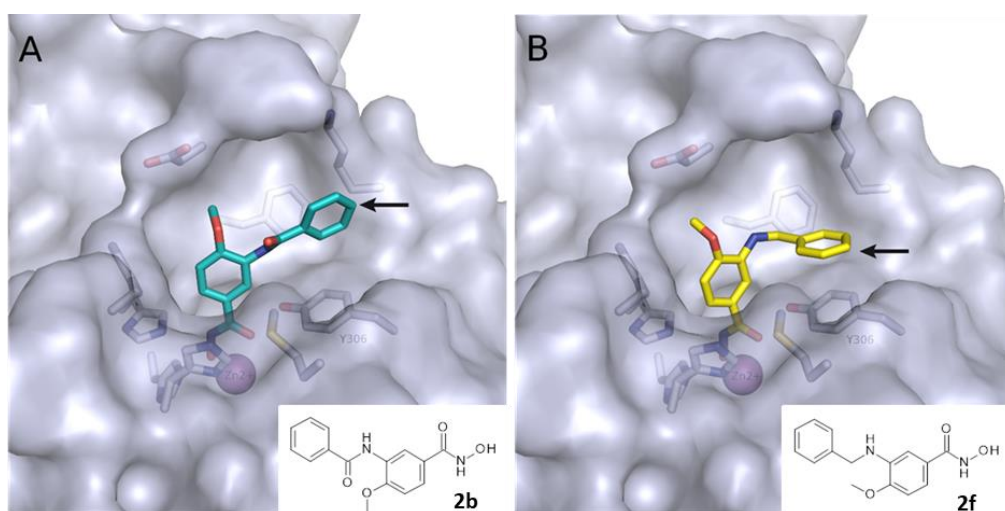
Figure 3 Predicted binding mode of A) **2b** (colored cyan) and B) **2f** (colored yellow) in human HDAC8 (PDB ID: 6ODB). The arrow indicates the point of linker attachment (*p*-position of the terminal phenyl ring).

The synthesized HDAC8 degraders were designed to act through PROTAC technology or HyT. In several studies, it was proven that the selectivity profile of bifunctional molecules towards protein isoforms that are closely related can be influenced by many factors including the E3 ligase recruited [54,55], the length of the linker [55-58], as well as the point of linker attachment on each of the recruiting units [55,59,60]. The reason is that the formation of the ternary complex is highly affected by these factors. In a trial to increase the probability of the engagement of a ligase by the developed degraders, we used two different ligands to recruit the two E3 ligases which are most utilized in degrader development: the cereblon (CRBN) ligand pomalidomide and a VHL ligand. We also used a variety of linkers, including PEG- and hydrocarbon-based linkers with varying lengths in addition to triazole ring containing linkers. The *in vitro* activity of the synthesized compounds against human HDAC enzymes as well as on neuroblastoma cells were determined.

Chemical synthesis of PROTACs and inhibitors

The synthesis of the HDAC degraders (**1a-p, Table 1B**) is summarized in **Schemes 1-6**. According to the nature of the linker, the para position of the phenyl cap group of the protected form of the hydroxamic acid based HDAC inhibitor was functionalized. .

To synthesize the degraders (**1a-c, 1k and 1m-o, Schemes 1-3**), the protected form of the hydroxamic acid based HDAC inhibitors were synthesized to contain an amino group or an aminomethyl group on the cap phenyl ring. These free amino groups were reacted with the respective carboxylic acid at the terminal part of the aliphatic linker of the E3 ligase ligand-linker-conjugates or adamantane-linker-conjugates (see

11

Scheme S4.1 in Supp. Info.) forming an amide bond. An exception is **1k** (**Scheme 2)** where the protected HDAC inhibitor was first linked to the linker through amidation, then the formed protected HDAC inhibitor-linker conjugate was reacted with the VHL ligand to form the protected PROTAC. Finally, the protecting group whether benzyl or 2-tetrahydropyranyl was removed to yield the free hydroxamic acid containing degraders.

For the synthesis of degrader molecules (**1d-f**, **Scheme 4**) an alkyne functional group was introduced to the protected form of the hydroxamic acid-based inhibitor. On the other hand, conjugates composed of pomalidomide attached through an amide bond to an aliphatic linker terminated with an azide group were synthesized (see **Scheme S4.2** in Supp. Info.). The two units were then attached via azide-alkyne Huisgen cycloaddition followed by deprotection of the tetrahydropyran protected hydroxamic acid to yield the bifunctional molecules.

In the degraders (**1g-j, 1l and 1p**) whose synthesis is demonstrated in **Schemes 5 and 6** the protected form of the hydroxamic acid based HDAC inhibitor was functionalized in the para position of the cap phenyl ring with a carboxylic acid group. This group was then reacted with the amino-group in the E3 ligase ligand/ HyT-linker conjugate to form an amide bond.
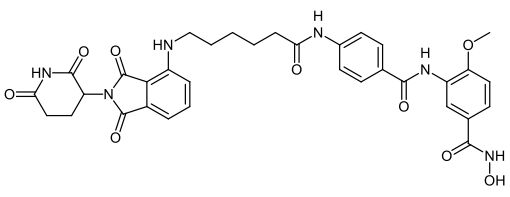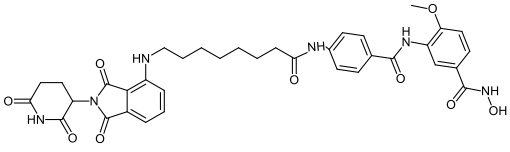
Scheme 6 displays the synthesis of degraders (**1i and 1j**). In the first trial of the deprotection step of the benzyl protected degrader through catalytic hydrogenation, Pd/C (10%) was used. This resulted in the unwanted removal of the chlor atom. Consequently, Pd/C (5%) was used in the subsequent deprotection trial which led to the retainment of the halogen. The unexpected degrader molecule formed was then
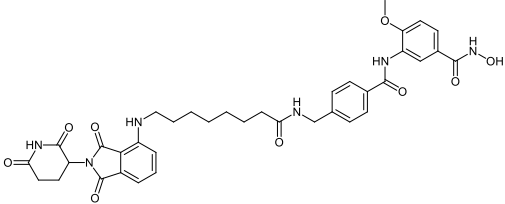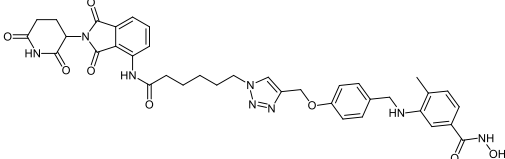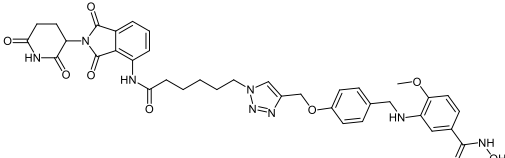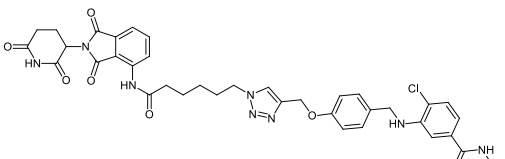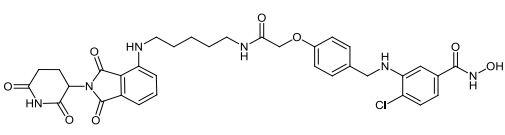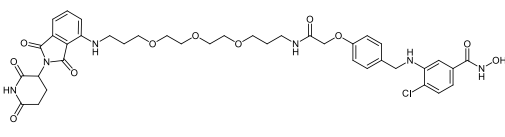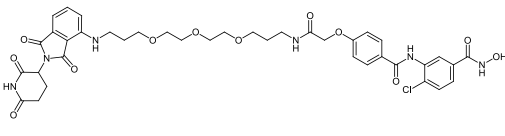
included in the testing to investigate the effect of the absence of the para-halogen atom on the degradation profile of the degrader.
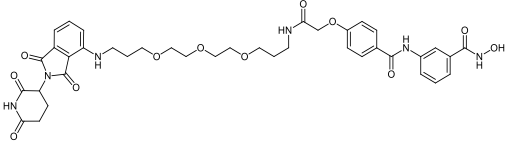
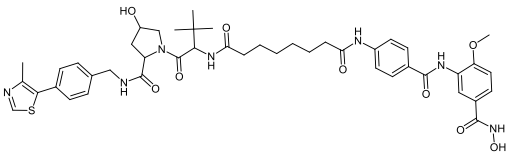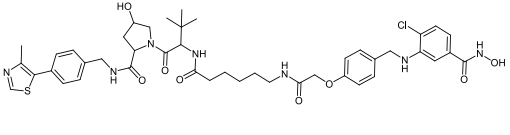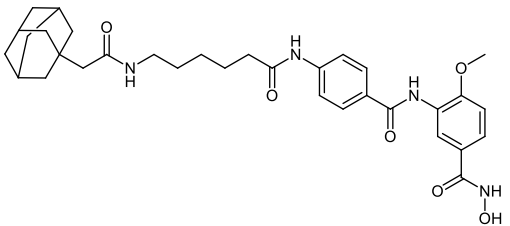In some synthesized degraders (eg. **1a and 1m**), the HDAC8 inhibitor and the linker were retained, while the entity interacting with the protein degrading machinery was changed. In other cases, both pharmacophores were kept unchanged while the length and/or nature of the linker was changed (eg. **1a and 1b; 1g and 1h**). Also, as shown in **Scheme 4** (**1d-f**) we synthesized compounds in which only the HDAC8 inhibitor was changed through different substitution. All these designs were aimed at creating a pool of compounds for the investigation of the effect of the different factors on the degradation ability of the synthesized degraders to optimize the design of a successful HDAC8 degrader.

In vitro testing using recombinant HDACs

Table 1A IC$_{50}$ values for synthesized PROTACs.

ID	Structure	HDAC1 IC$_{50}$ (µM)	HDAC6 IC$_{50}$ (µM)	HDAC8 IC$_{50}$ (µM)
	CRBN-based PROTACs			
1a		4.37 ± 0.65	0.22 ± 0.06	0.09 ± 0.03
1b		>20	0.56 ± 0.1	0.81 ± 0.17

13

1c		10 μM: 40.1 1 μM: 22.2	0.25 ± 0.02	0.15 ± 0.01
1d		13.1 ± 0.6	6.7 ± 0.6	0.37 ± 0.05
1e		16.2 ± 0.8	17.2 ± 2.4	0.25 ± 0.07
1f		10.8 ± 0.7	1.3 ± 0.3	0.25 ± 0.03
1g		10 μM: 69% 1μM: 10.1%	10 μM: 72.6% 1μM: 24.8%	0.59 ± 0.11
1h		3.91 ± 0.48	10 μM: 66.8% 1μM: 33.5%	0.33 ± 0.19
1i		10 μM: 67.4% 1μM: 20.7%	10 μM: 92.3% 1μM: 85.4%	0.65 ± 0.14

1j		10 μM: 60.0% 1μM: 13.9%	10 μM: 80.9% 1μM: 46.2%	4.84 ± 1.05
	VHL-based PROTACs			
1k		>20	0.31 ± 0.01	0.11 ± 0.01
1l		10 μM: 45.5% 1μM: 6.0%	10 μM: 72.4% 1μM: 8.3%	0.72 ± 0.15
	HyT-based PROTACs			
1m		10 μM: 81.9% 1μM: 47.7%	0.25 ± 0.08	0.57 ± 0.11
1n		10 μM: 30.0% 1 μM: 38.6%	0.82 ± 0.05	0.39 ± 0.03
1o		10 μM: 52.6% 1 μM: 9.8%	0.37 ± 0.03	0.09 ± 0.01

ID	Structure			
1p		10 µM: 40.0% 1µM: 2.3%	10 µM: 72.8% 1µM: 12.4%	0.75 ± 0.09

Table 1B IC_{50} values for benzhydroxamate-based HADC inhibitors underlying

PROTAC development.
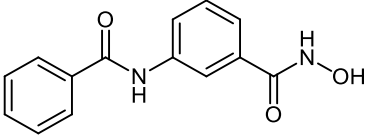
ID	Structure	HDAC1 IC_{50} (µM)	HDAC6 IC_{50} (µM)	HDAC8 IC_{50} (µM)
2a		33.6 ± 1.8	3.0 ± 0.3	0.58 ± 0.05
2b		2.3 ± 1.2	2.5 ± 1.1	0.09 ± 0.02
2c		11.6 ± 3.9	0.12 ± 0.02	0.12 ± 0.04
2d		2.3 ± 1.2	2.5 ± 1.1	0.14 ± 0.01
2e		21.8 ± 2.1	5.1 ± 0.3	0.26 ± 0.04
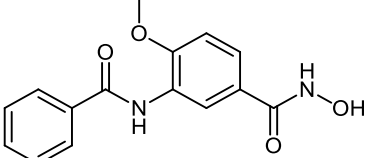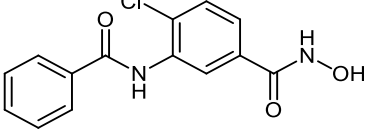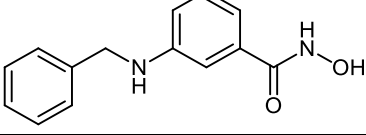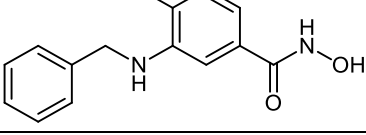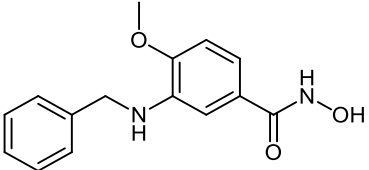
2f		14.5 ± 1.4	5.1 ± 0.8	0.07 ± 0.02
2g		10.4 ± 1.2	4.0 ± 0.2	0.25 ± 0.04
2h		>20	0.15 ± 0.001	0.01 ± 0.001
2i		>20	7.4 ± 0.6	0.41 ± 0.05
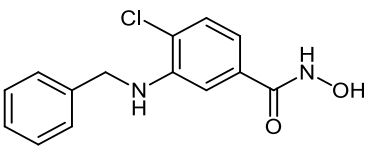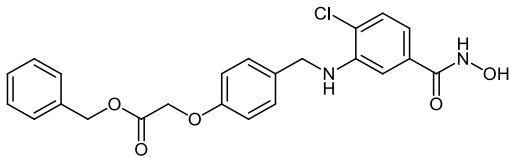
In vitro testing for HDAC-inhibition (**Table 1**, see Methods section for details) using recombinant HDACs and the peptidic Fluor-de-Lys as substrate showed that the synthesized degraders having 4-substituted 3-aminobenzhydroxamates (e.g. **1d-f**) as HDAC inhibitor part exhibited preference for HDAC8 over the other tested human HDACs (HDAC1 and 6) as shown in **Table 1B**. However, degraders possessing 4-substituted 3-amidobenzhydroxamates (e.g. **1b** and **1c**) as warhead showed comparable inhibitory activity against HDAC6 and 8 (**Table 1A**).

While CRBN-based PROTACs **1a-c** were designed on the basis of the potent HDAC8 inhibitor **2b**, **1d-f** were synthesized based on the potent HDAC8 inhibitors **2e**, **2f** and **2h** and **2g** respectively. The difference between the degraders **1a-c** is in the length of the linker. While in **1a** there is a six-carbon amide linker attached to the

target binding unit, in **1b** the linker is eight carbon long. In the case of **1c**, the unit linking the inhibitor and the E3 ligase part is elongated via the functionalization of the cap group of the inhibitor with aminomethyl group instead of amine group as in **1b**. The HDAC8 inhibitory activity was comparable to the parent inhibitor, in the case of **1a** (SI (HDAC6/HDAC8) = 2) and **1c** (SI (HDAC6/HDAC8) = 2). It decreased in the case of **1b** (SI (HDAC6/HDAC8) = 0.7) but remained in the submicromolar range. On the other hand, the selectivity over HDAC6 decreased in the three PROTACs compared to **2b** (SI (HDAC6/HDAC8) = 28).

While **1a-c** possess a hydrocarbon chain as a linker, **1d-f** have a triazole containing linker [28]. **1d** (SI (HDAC6/HDAC8) = 18) and **1e** (SI (HDAC6/HDAC8) = 69) maintained a significant selectivity over HDAC6, while the selectivity of **1f** over HDAC6 (SI (HDAC6/HDAC8) = 5) was found to be 3-fold lower than its parent inhibitor **2g** (SI (HDAC6/HDAC8) = 16).

The pomalidomide-based PROTACs **1g** and **1h** were based on the inhibitor **2e**. Degraders **1g** and **1h**, which only differ in the type of the linker used, showed an almost equipotent activity as the parent inhibitor and significant selectivity over HDAC6. The difference between degrader molecules **1i**, which was designed based on inhibitor **2c**, and **1j** is the absence of the chloro-substituent at position-4 of the benzhydroxamic acid. **1j** is the result of reductive dechlorination which took place during the synthesis of **1i**. The HDAC8 activity was greatly affected and changed from the nanomolar range to the micromolar range further confirming the importance of para-substitution for HDAC8 inhibitory activity. This observation was in accordance with our previous reports [52,16] and further confirm the importance of the para-substitution for HDAC8 inhibitory activity.

1k and **1b** differ in the degradation machinery recruiting unit. While **1k** (SI (HDAC6/HDAC8) = 3) has a VHL-ligand as the E3 ligase binding unit, **1b** (SI (HDAC6/HDAC8) = 0.7) bears the CRBN-warhead pomalidomide. Both degraders showed an HDAC8 inhibitory activity with the IC_{50} values in the submicromolar range. The selectivity over HDAC6 was however lost compared to the parent inhibitor **2b** (SI (HDAC6/HDAC8) = 28).

1m-p possess adamantane as the degrading machinery engaging unit. In **1m-o** the linker is extended through amide formation with an acetic acid handle bound to the adamantane. In **1o** (SI (HDAC6/HDAC8) = 4) an elongation of the linker is achieved through the aminomethyl functionalization of the inhibitor's cap group as compared with **1n** (SI (HDAC6/HDAC8) = 2). This elongation resulted in an inhibitory activity on HDAC8, comparable to the parent inhibitor **2b** and was accompanied with a 2-fold increase in the selectivity over HDAC6 compared to **1n**. As their pomalidomide based counterparts **1a-c**, **1m-o** demonstrated good inhibitory activity towards HDAC8 and a significant decrease in the selectivity over HDAC6 compared to the parent inhibitor **2b** (SI (HDAC6/HDAC8) = 28).

Interestingly, the addition of the methylene group between the amide group and the cap group of the inhibitor in **1c** and **1o** resulted in the improvement of the inhibitory activity against HDAC8 in comparison with **1b** and **1n** respectively, so that the IC_{50} values of **1c** and **1o** were similar to that determined for **2b**. Although different ligands for the degrading machinery and different linkers were employed in **1l** and **1p**, both displayed equal inhibitory activity towards HDAC8 and significant selectivity over HDAC6.

Collectively, all synthesized PROTACs, with the exception of the *p*-unsubstituted derivative **1j**, showed HDAC8 inhibitory activity in the submicromolar range which should guarantee the ability of the bifunctional molecules to bind to HDAC8. In addition, the inhibition of HDAC1 was found to be weak. The negative control **33** (see **S2** in Supp. Info.) which possesses a carboxylic ester group instead of the hydroxamic acid group did not demonstrate a strong inhibitory activity against any of the tested HDACs. This confirms the necessity of the presence of a zinc binding group, in this case the hydroxamic acid group, for the degraders/inhibitors to bind to the HDAC enzymes.

Schemes:
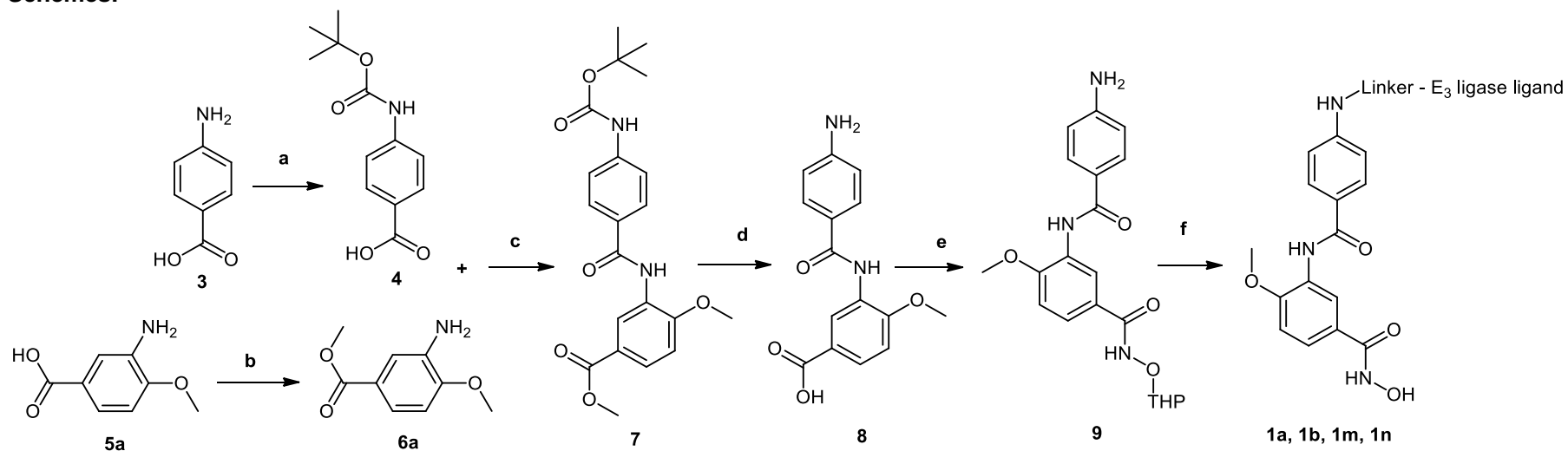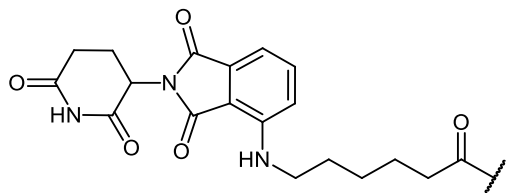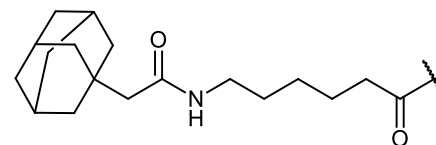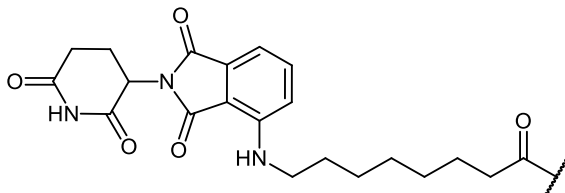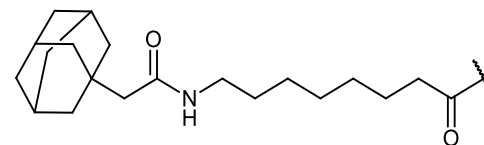
Scheme 1: Reagents and conditions: (a) TEA, Boc₂O, 1,4-dioxane, H₂O, room temperature, 24h; (b) MeOH, SOCl₂, reflux, 3h; (c) DIPEA, HATU, DMF, 50°C, 24h; (d) 1) 1M NaOH, MeOH, reflux, 2h; 2) TFA, DCM, room temperature, 2h; (e) DIPEA, HATU, NH₂OTHP, DMF, 50°C, 24h; (f) 1) E3 ligase ligand-linker-COOH **43a,b** / HyT-linker-COOH **47a,b** (see **Scheme S4.1** in Supp. Info.), DIPEA, HATU, DMF, 50°C, 24h; 2) 1M HCl, THF, US, room temperature, 2h.
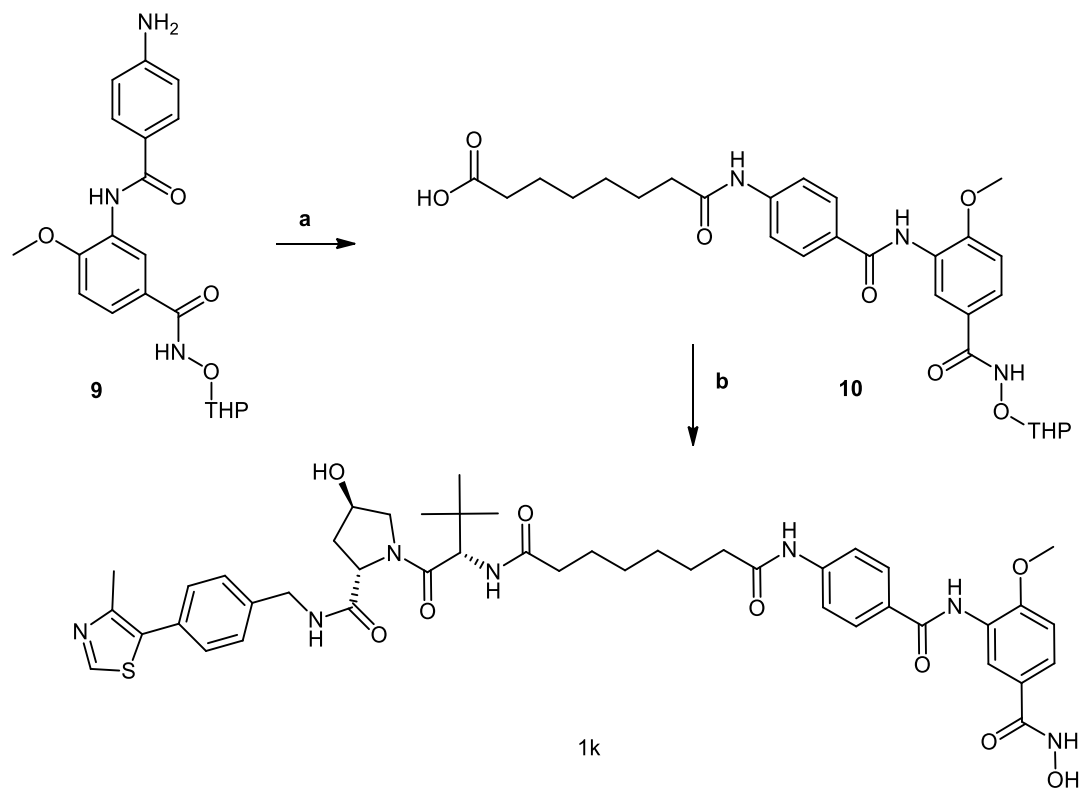
Scheme 2: Reagents and conditions: (a) Suberic acid, NMI, TCFH, ACN, room temperature, 24h; b) 1) VHL ligand **40** (see **S3** in Supp. Info.), DIPEA, HATU, DMF, 0°C, 2h; 2) 1M HCl, THF/MeOH, US, 0°C, 2h.
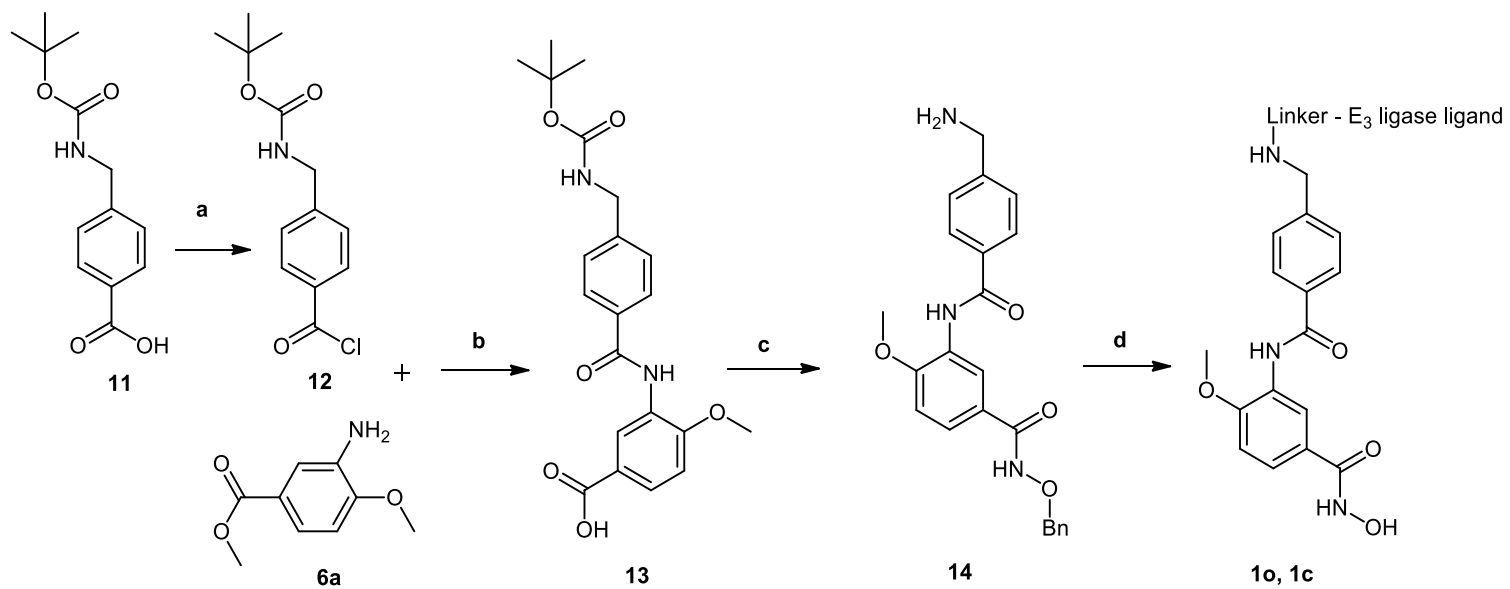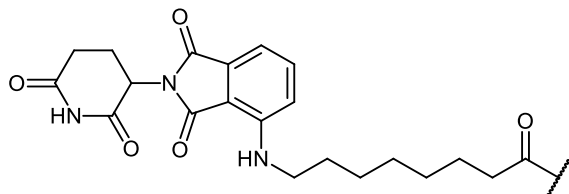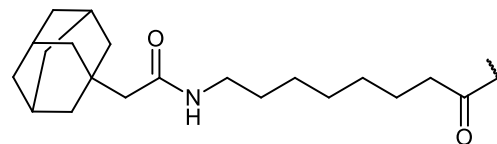
Scheme 3: Reagents and conditions: (a) DMF, C_5H_5N, $C_2O_2Cl_2$, room temperature, 6h; (b) 1) C_5H_5N, room temperature, 24h; 2) 1M NaOH, MeOH, reflux, 2h; (c) 1) DIPEA, HATU, $NH_2OBn·HCl$, DMF, 50°C, 24h; 2) TFA, DCM, room temperature, 2h; (d) 1) E3 ligase ligand-linker-COOH **43b** / HyT-linker-COOH **47b** (see **Scheme S4.1** in Supp. Info.), DIPEA, HATU, DMF, 50°C, 24h; 2) Pd/C (5%), H_2, THF, 24h.
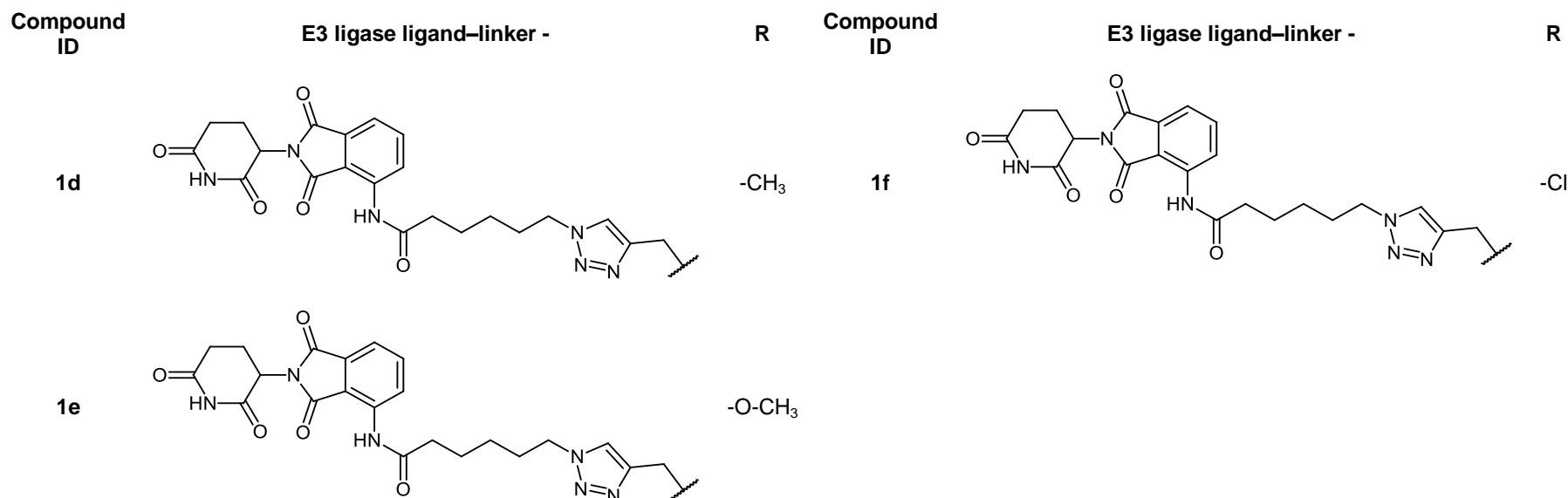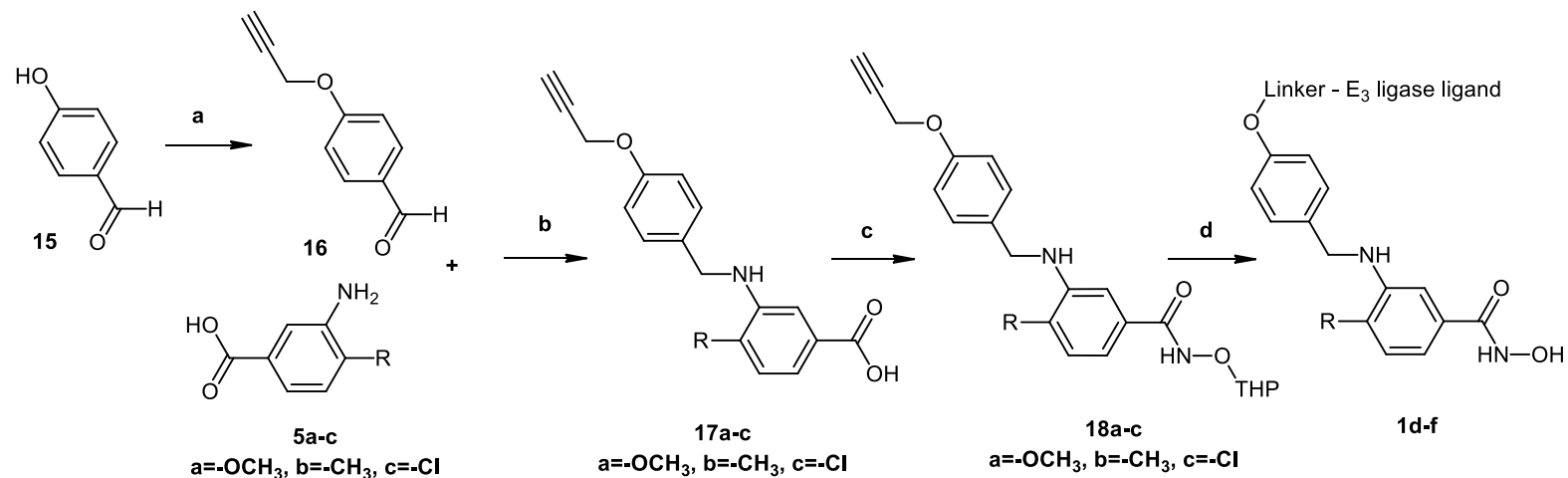
Scheme 4: Reagents and conditions: (a) 1) K_2CO_3, DMF, room temperature, 1hr; 2) propargyl bromide at 0°C; 3) 24hrs at room temperature; (b) 1) toluene, reflux, 2hr; 2) THF, 0°C, CH_3COOH, $Na(CH_3COO)_3BH$, 30min; 3) 24h, room temperature; (c) DIPEA, HATU,NH_2OTHP, DMF, 50°C, 24h; (d) 1) E3 ligase ligand-linker-N_3 **50** (see **Scheme S4.2** in Supp. Info.), tert-Butanol / H_2O, Sod. Ascorbate, $CuSO_4$ x $5H_2O$, 24h, room temperature; 2) 1M HCl, THF, US, room temperature, 2h.
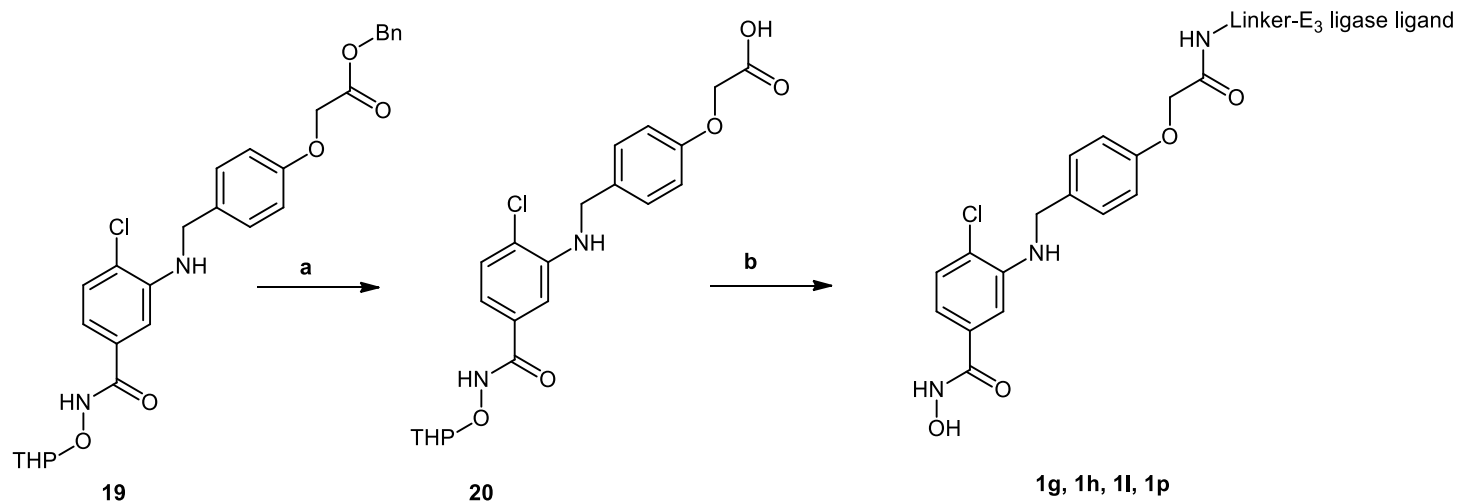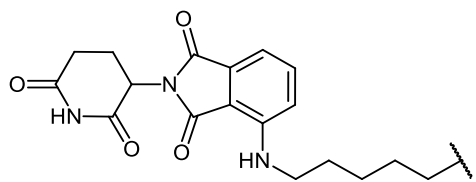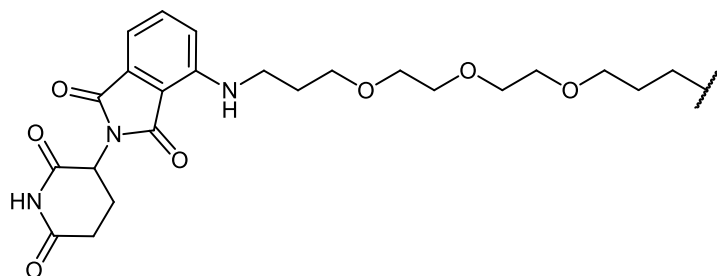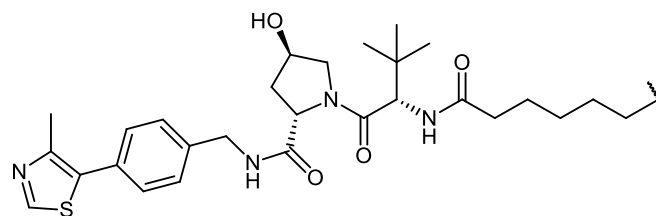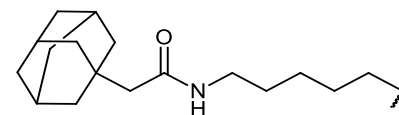
Scheme 5: Reagents and conditions: (a) Pd/C (5%), H₂, EtOAc: THF (1:1); (b) 1) E3 ligase ligand-linker-NH₂ **53, 56, 59** / HyT-linker-NH₂ **57** (see **Scheme S4.3** in Supp. Info.), DIPEA, HATU, DMF, room temperature; 2) 2M HCl, THF, room temperature.
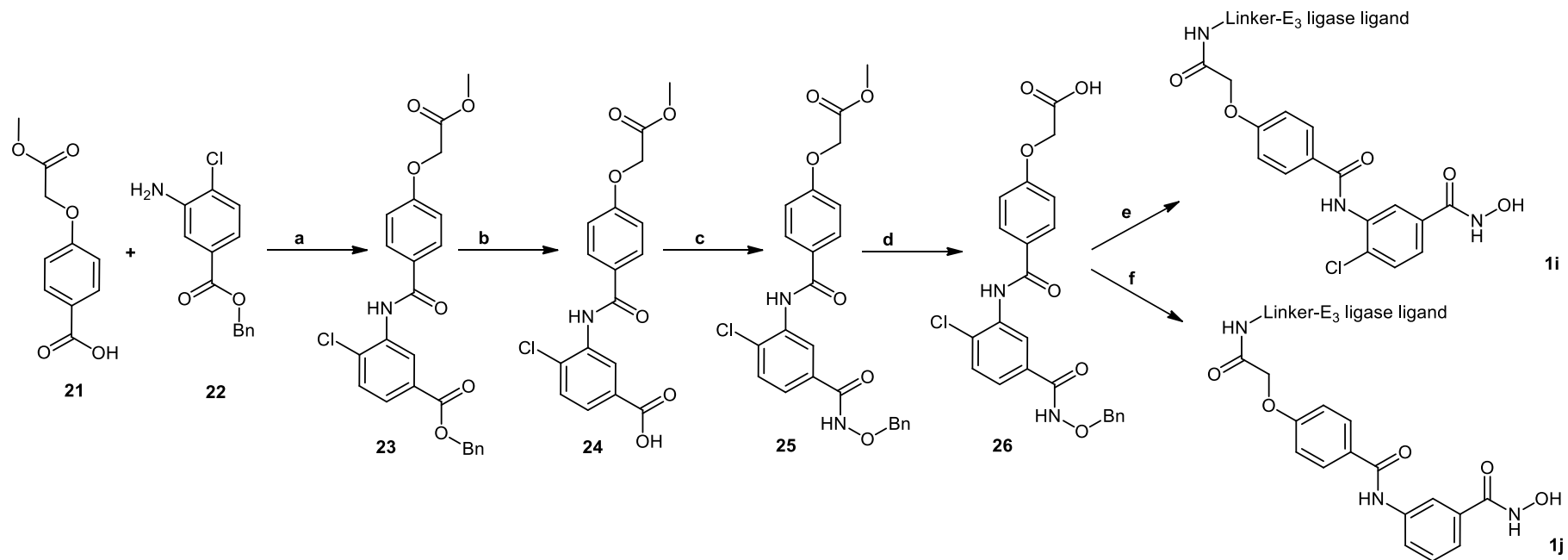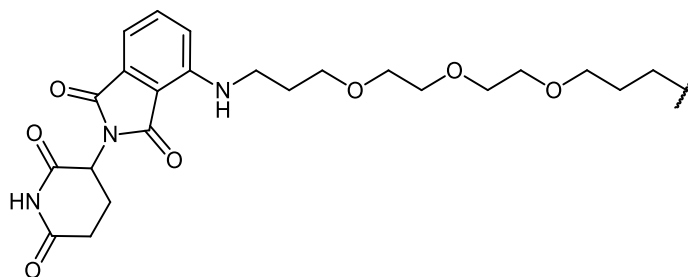
Scheme 6: Reagents and conditions: (a) 1) SOCl$_2$, reflux, 2) DIPEA, THF; (b) Pd/C (5%), H$_2$, EtOAc: THF (1:1); (c) DIPEA, HATU, NH$_2$OBn·HCl, DMF, room temperature; (d) LiOH, H$_2$O: THF (1:1), room temperature; (e) 1) E3 ligase ligand-linker-NH$_2$ **53** (see **Scheme S4.3** in Supp. Info.), HATU, DIPEA, DMF; 2) H$_2$, Pd/C (5%), MeOH. (f) 1) E3 ligase ligand-linker-NH$_2$ **53** (see **Scheme S4.3** in Supp. Info.), DIPEA, HATU, DMF; 2) H$_2$, Pd/C (10%), MeOH.

Cytotoxicity assay

HDACi should have low toxicity to normal mammalian cells. To test the potential toxicity of the *in vitro* active PROTACs, cytotoxicity tests were performed on human embryonic kidney-derived HEK293 cells. The cells were incubated for 48 h with the PROTACsi at a concentration of 50 μM, and cell viability was determined by the Alamar Blue assay. As shown in **Table 2**, the HDAC8 inhibitors and PROTACs showed weak to no cytotoxic effects against HEK293 cells at the used concentration of 50 µM.

Table 2 Cytotoxicity on HEK293 cells (cell viability at 50 μM inhibitor treatment)**.**

ID	HEK293 viability 50 µM	ID	HEK293 viability 50 µM	ID	HEK293 viability 50 µM
2a	72.0 ± 2.9	1a	85.6 ± 2.4	1j	83.7 ± 3.5
2b	67.3 ± 3.9	1b	64.1 ± 1.7	1k	78.2 ± 3.7
2c	72.2 ± 3.5	1c	70.1 ± 6.7	1l	90.4 ± 2.3
2d	78.8 ± 6.1	1d	80.2 ± 2.8	1m	51.5 ± 6.2
2e	90.4 ± 1.7	1e	65.1 ± 4.3	1n	60.0 ± 3.7
2f	68.1 ± 1.2	1f	100.5 ± 2.8	1o	69.3 ± 1.2
2g	87.4 + 3.4	1g	68.2 ± 2.5	1p	80.1 ± 1.9
2h	70.4 ± 7.5	1h	61.3 ± 0.9		
2i	88.1 ± 0.1	1i	97.6 ± 7.0		

Testing on neuroblastoma cells

In order to measure the functional consequence of HDAC8 inhibition, two different cell lines were used, SK-N-BE(2)-C cells which display MYCN amplification and non-functional p53 as well as IMR32 cells having p53 wild type, which both respond with growth arrest and signs of neuronal differentiation upon knockdown or selective inhibition of HDAC8. Growth arrest was determined by colony formation and viability assays. Cells were treated with 5 and 10 µM of each of the CRBN based HDAC8 PROTACs having a triazole linker (**1d, 1e, 1f**) for 96 h, followed by culturing for another 6 days without treatment (**Figure 4A**). This assesses whether the treatment impairs the clonogenic growth capacity of tumor cells, indicating effectiveness of compounds on the survival and proliferation of tumor cells. **1d** and **1e** showed strongest effect on the colony formation whereas the related analog **1f** was found to be inactive. The HDAC8 inhibitor **33** was used in comparison and showed a weak effect.

Moreover, we treated neuroblastoma IMR32 cells with the remaining PROTACs and counted the resulting viable cells. We quantified the percentage of dead cells as shown in (**Figure 4B-C**). In addition, cell proliferation was assessed via counting of viable cells (**Figure 4D-E**). The CRBN PROTAC **1b** and the HyT PROTAC **1p** significantly decreased the ability to form colonies at 5 and 10 µM concentrations and showed also the strongest effect in the cell proliferation assay. In case of **1k** and **1m** the results were less significant whereas the remaining PROTACs were all found to be inactive. As reference, the HDAC8 inhibitor PCI-34501 was used [16].
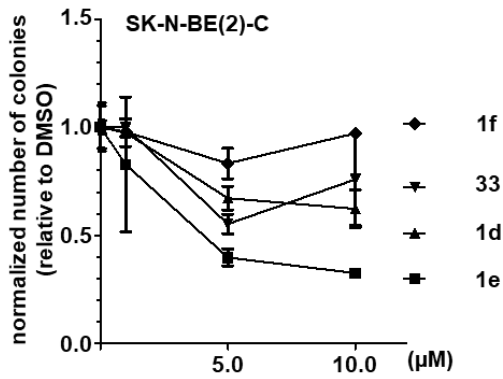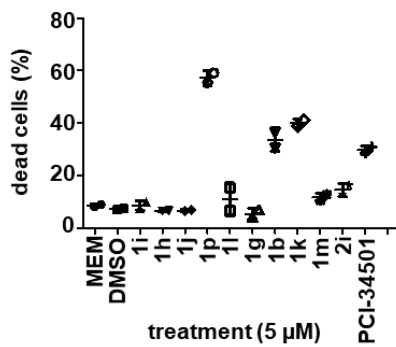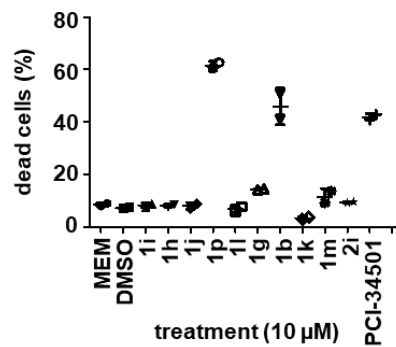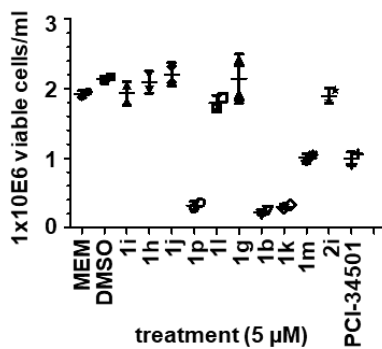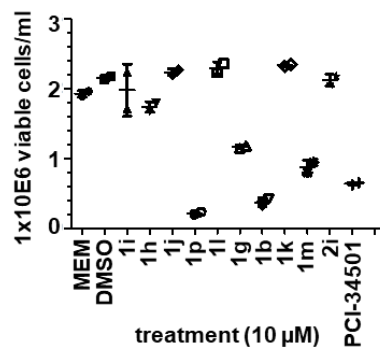
Figure 4 A) Neuroblastoma SK-N-BE(2)-C cells; Colony Assay, 10 days (compound treatment within first 96h). Stained with crystal violet and quantified with ImageJ. **B-C)** Trypan Blue assay for detection of dead cells. Neuroblastoma IMR-32 cells were either treated with 5 µM **(B)** or 10 µM **(C)**. **D-E)** Cell proliferation assessed via counting of viable cells. IMR-32 cells were either treated with 5 µM **(D)** or 10 µM **(E)**

PROTACs. HDAC8i PCI-34501 served as a positive control, untreated (MEM) and solvent (DMSO) treated cells as negative controls.

To test the degradation of HDAC8 with the developed PROTACs, we selected the most promising compounds obtained from the cellular neuroblastoma testing, namely **1b**, **1d**, **1e**, **1m** and **1p**. Whole cell lysates from treated SK-N-BE(2)-C neuroblastoma cells were taken and the protein levels for HDAC8 and the acetylation of its substrate SMC3 were determined (**Figure 5**). As a control for HDAC6, we also assessed acetylation levels of α-tubulin. It revealed that 6h treatment and a concentration of 10 µM gives the highest degradation of HDAC8 for the CRBN based PROTACs **1b** and **1e** in SK-N-BE(2)-C cells (**Figure 5A, 5B**). The CRBN PROTAC 1b resulted in 40% remaining HDAC8 protein whereas CRBN PROTAC 1e reduced HDAC8 down to 30% protein level. Both PROTACs showed also a strong hyperacetylation of the HDAC8 substrate SMC3. As expected, the negative control **33** (bearing a carboxyl ester instead of the hydroxamic acid) did not show hyperacetylation of SMC3 or HDAC8 degradation. Also, the CRBN POTAC **1d,** and the HyT PROTACs **1m** and **1p** failed to degrade HDAC8 in this neuroblastoma cell line (**Figure 5A-B**). We also tested the most potent PROTACs **1b** and **1e** whether they are able to degrade HDAC1 or HDAC6 (**Figure 5C**) but none showed a significant effect at the highest concentration of 10 µM. Thus the active HDAC8 degraders **1b** and **1e** are selective and do not degrade HDAC1 and HDAC6.
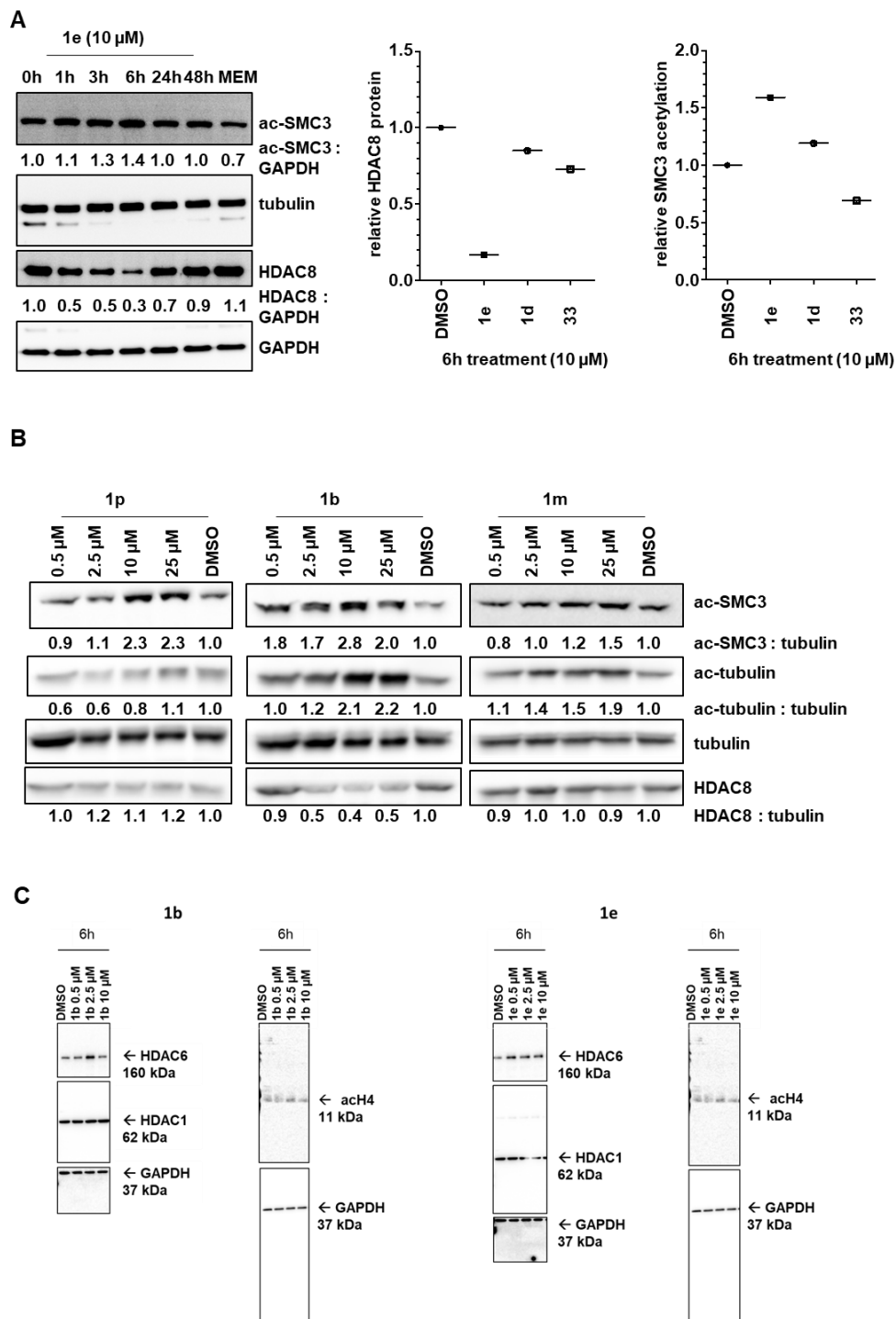
Figure 5: A) SK-N-BE(2)-C neuroblastoma cells were treated for indicated time points with 10 μM of PROTACs. Degradation of HDAC8 and acetylation of HDAC8

target was analysed via western blot. B) SK-N-BE(2)-C neuroblastoma cells were treated for 6h with **1b, 1p** and **1m** at the concentrations given in the figure. Degradation of HDAC8 and acetylation of HDAC8 target SMC3 as well as acetylation of HDAC6 target tubulin was analysed via western blot. C) SK-N-BE(2)-C neuroblastoma cells were treated for 6h with PROTACs **1b** and **1e**. Degradation of HDAC1 and HDAC6 as well as substrate acetylation was analysed at given concentration via western blot.

As HDAC8 inhibition is known to induce signs of neuronal differentiation, such as neurite-like outgrowths in neuroblastoma cells [6]), we treated SK-N-BE(2)-C cells with **1b, 1e**, **1m** and PCI-34051 for 6-10 days then stained the cells with crystal violet to visualize neurite-like outgrowths. For comparison, we treated the cells with the known neuronal differentiation inducer retinoic acid (ATRA) which is a known drug, that is applied for neuroblastoma treatment under some circumstances. We also combined one PROTAC, namely **1e** with ATRA, which substantially enhanced the differentiation phenotype (**Figure 6**). These results are in line with the published differentiation enhancement (longer outgrowths, more cells with outgrows in combination) effect of HDAC8 inhibitors such as PCI-34051 [6].

A

solvent

10 µM 1e

10 µM ATRA

10 µM 1e + 10 µM ATRA

B

DMSO

5 µM 1b

5 µM PCI-34051

5 µM 1m
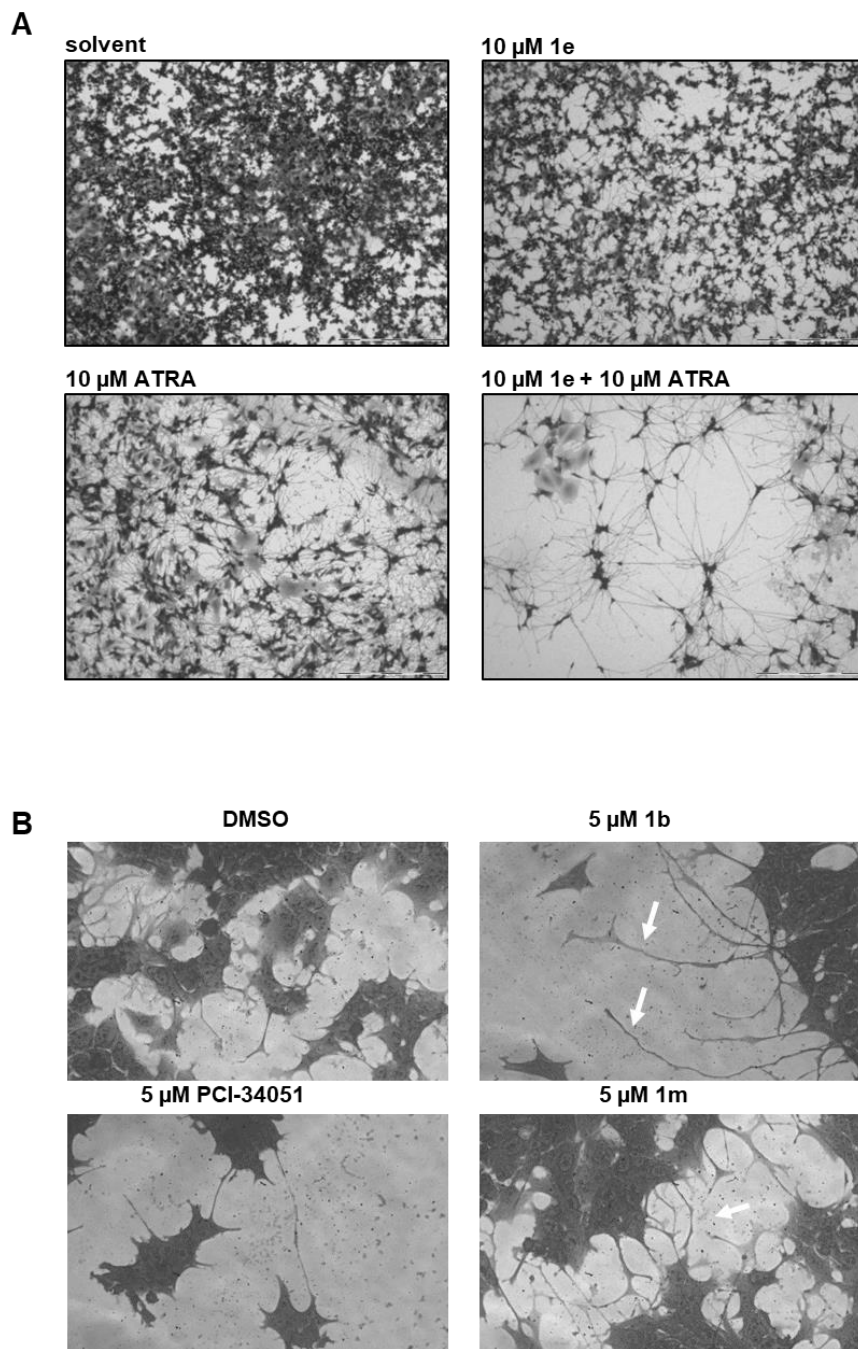
Figure 6: A) SK-N-BE(2)-C cells, treated for 10 days. Scale bar: 500 µm. Stained with crystal violet. B) SK-N-BE(2)-C cells, treated for 6 days. Stained with crystal violet.

Conclusion

In summary, we designed a pool of bifunctional PROTACs based on previously published HDAC8 inhibitors with good inhibitory activity. Different linker types and lengths in addition to various degradation machinery recruiting units were employed. The effect of these factors on the degradation ability of the synthesized PROTACs was demonstrated through testing them on SK-N-BE(2)-C neuroblastoma cells and determination of the protein levels for HDAC8 and the acetylation level of its substrate SMC3. From the synthesized compounds only the CRBN based PROTACs **1b** and **1e** resulted in strong HDAC8 degradation connected with SMC3 acetylation. The synthesized VHK and HyT based PROTACs did not show significant HDAC8 degradation. Testing of the active PROTACs **1b** and **1e** against HDAC1 and HDAC6 (substrate acetylation as well as degradation) showed no effects confirming the good selectivity of these compounds. Besides the good HDAC8 degradation effects of the degraders **1b** and **1e**, these two compounds also exhibited good anti-neuroblastoma activity and showed enhancing of the differentiation phenotype. Overall, the PROTACs developed represent useful tools to investigate the physiological functions of HDAC8 in other cancer cells in future studies.

I.   Materials and methods

1.   General

All materials and reagents were purchased from Sigma-Aldrich Co. Ltd. and abcr GmbH. All solvents were analytically pure and were dried before use. Thin layer chromatography was carried out on aluminium sheets coated with silica gel 60 F254 (Merck, Darmstadt, Germany). For medium pressure chromatography (MPLC) silica gel Biotage® SNAP ultra-HP-sphere 25 µm containing columns were used.

Chloroform:methanol; n-hexane:ethyl acetate or ethyl acetate:acetonitrile were the elution systems used for medium pressure chromatography. Triethyl amine was added in a concentration of 0.1 % to chloroform or ethyl acetate, according to the solvent system used, in purification of compounds protected with 2-tetrahydropyranyl group.

In the preparative high-pressure chromatography used for cleaning of the final PROTACs, LiChrosorb® RP-18 (7 µm) 250-25 Merck column was used. The applied mobile phase was a gradient with increasing polarity composed of acetonitrile/water.

Final compounds´ purity was determined using high-pressure chromatography (HPLC). Purity was measured by UV absorbance at 254 nm. Two analytical methods were used while determining the purity. In the first method (M1), the components of the HPLC were an XTerra RP18 column (3.5 mm, 3.9 mm x 100 mm) from the manufacturer Waters (Milford, MA, USA) and two LC-10AD pumps, a SPD-M10A VP PDA detector, and a SIL-HT autosampler, all from the manufacturer Shimadzu (Kyoto, Japan). In the second method (M2), only the column was changed to LiChrosorb® RP-18 (5 µm) 100-4.6 Merck column.

Mass spectrometry analyses were performed with a Finnigan MAT710C (Thermo Separation Products, San Jose, CA, USA) for the ESIMS spectra and with an LTQ (linear ion trap) Orbitrap XL hybrid mass spectrometer (Thermo Fisher Scientific, Bremen, Germany) for the HRMS-ESI (high resolution mass spectrometry) spectra. For the HRMS analyses, the signal for the isotopes with the highest prevalence was given and calculated (^{35}Cl, ^{79}Br).

^{1}H NMR and ^{13}C NMR spectra were taken on a Varian Inova 500 using deuterated chloroform or deuterated dimethylsulfoxide as solvent. Chemical shifts are referenced to the residual solvent signals.

Non-enzymatic stability of selected final compounds was determined using 10 µM concentration of the tested PROTACs in one of the following assay media; Dulbecco's Modified Eagle Medium (DMEM) (50%)/ Dimethylsulfoxid (10%)/ acetonitrile (40%) or DMEM (50%)/ Dimethylsulfoxid (10%)/ methanol (40%) mixture at pH7.4. In case of TH166 Methanol was used instead of acetonitrile due to solvent problems. The formed solution mixtures were incubated for 0, 6, 12, 24, 48 and 72h at 37°C. Analyte decomposition was monitored by HPLC using XTerra RP18 column (3.5 mm, 3.9 mm x 100 mm) from the manufacturer Waters (Milford, MA, USA) and two LC-10AD pumps, a SPD-M10A VP PDA detector, and a SIL-HT autosampler, all from the manufacturer Shimadzu (Kyoto, Japan).

2.   General synthetic methods

Method I, reductive amination

 A. A mixture of the benzaldehyde (1 eq.) and the amine (5% molar excess) was dissolved in toluene and was heated under reflux using a water trap for 2h. Afterwards the solvent was removed under reduced pressure. The remaining

residue was dissolved in dry tetrahydrofuran and the formed solution was cooled to 0°C. Glacial acetic acid (2 eq.) was added followed by sodium triacetoxyborohydride (4 eq.) and the reaction mixture was stirred for 30 minutes at 0°C. Afterwards the ice bath was removed and stirring was continued for 24h at room temperature. The reaction was then quenched by the addition of sodium bicarbonate and the product was extracted with ethyl acetate. The organic layer was washed with 1M hydrochloric acid followed by brine and was dried over anhydrous sodium sulfate. Finally, it was filtered and evaporated under reduced pressure. The crude product was purified using the MPLC. The yields were in the range 60%-95%.

B. A mixture of benzaldehyde (1.1 eq.), the corresponding amine (1 eq.), trifluoroacetic acid (2 eq.), and sodium triacetoxyborohydride (1.2 eq.) was dissolved in a mixture of tetrahydrofuran and ethyl acetate (1:1). After stirring the reaction mixture at room temperature for 2h, the reaction was quenched by adding water and the crude product was extracted with ethyl acetate. The combined organic layer was dried over anhydrous sodium sulfate, filtered, and concentrated in vacuo. The crude residue was purified using MPLC. The yield was around 50%.

Method II, ester hydrolysis

A. To a solution of the methyl ester (1 eq.) in methanol, 1M aqueous sodium hydroxide (10 eq.) was added. The formed reaction mixture was refluxed for 2-4h. After complete ester hydrolysis, the solvent was evaporated under reduced pressure to yield a crude residue that was dissolved in water. The aqueous solution was extracted using ethyl acetate to remove any organic impurities. In the next step, 1M aqueous hydrochloric acid (10 eq.) was added to the aqueous

solution to liberate the free acid which was extracted using ethyl acetate. The combined organic layer was washed with brine and dried over anhydrous sodium sulfate. It was then filtered, and the solvent was evaporated under reduced pressure to give the crude product which was purified using the MPLC. The yields were 70%-96%.

B. To the suspension of the methyl ester (1 eq.) in a mixture of tetrahydrofuran and water (1:1) lithium hydroxide (5 eq.) was added. The mixture was stirred at room temperature until complete hydrolysis of the ester then tetrahydrofuran was evaporated. Using aqueous 1M hydrochloric acid, the pH of the remaining aqueous solution was adjusted to pH 6. The liberated free acid was extracted using a mixture of ethyl acetate and tetrahydrofuran. The combined organic layer was then dried over anhydrous sodium sulfate, filtered, and concentrated in vacuo to yield the product, which required no further purification. Crude yields were around 80-90%.

Method III, amide bond formation

A. A solution of the carboxylic acid (1-1.2 eq.) and *N,N*-diisopropylethylamine (3 eq.) in dimethylformamide was stirred for 15 min at room temperature then 1-[bis(dimethylamino)methylene]-1H-1,2,3-triazolo[4,5-b] pyridinium 3-oxid hexafluorophosphate (1.2-1.5 eq.) was added and stirring was continued for another 30 min. Next, the corresponding amine (1-1.5 eq.) was added to the solution. The formed reaction mixture was stirred at 0°C or at room temperature or at 50°C for 2-24h. After completion of the reaction, water was added to the reaction mixture and the formed solution was extracted using ethyl acetate. The combined organic layer was washed with aqueous 1M sodium bicarbonate solution followed by aqueous 1M ammonium chloride solution and brine. After

drying over anhydrous sodium sulfate, the organic layer was filtered then concentrated in vacuo to yield the crude compound which was purified using MPLC. The yields were around 27-100%.

B. To a suspension of the carboxylic acid (1 eq.) in toluene, drops of dimethylformamide were added followed by pyridine then oxalyl chloride (2 eq.). The reaction mixture was stirred at room temperature for 6h. The formed precipitate was then filtered and washed with toluene. Afterwards, the combined organic filtrates were concentrated under reduced pressure to give the acid chloride that was used directly without further purification. It was dissolved in pyridine and the amine (1 eq.) was added to the solution. The formed reaction mixture was stirred at room temperature for 24h. After evaporation of the solvent the remaining residue was dissolved in chloroform and was successively washed with 10% hydrochloric acid, 1M sodium bicarbonate and brine. After drying the organic layer over anhydrous sodium sulfate, it was evaporated under reduced pressure to give the crude product which was purified using the MPLC. The yield was around 48%.

C. After the dropwise addition of thionyl chloride (3 eq.) to the carboxylic acid (1 eq.) at 0 °C, the reaction mixture was heated under reflux for 2h then the excess thionyl chloride was evaporated under vacuum. The formed acid chloride was dissolved in dry tetrahydrofuran and was added dropwise to a solution of the corresponding amine (0.9 eq.) and N,N-diisopropylethylamine (3 eq.) in tetrahydrofuran. The reaction mixture was stirred at room temperature till completion. Afterwards it was diluted with ethyl acetate and was washed with a saturated aqueous solution of ammonium chloride followed by brine. Finally, the organic layer was dried over anhydrous sodium sulfate, filtered, and concentrated

in vacuo to obtain the crude residue which was purified using MPLC. The yield was around 50-70%.

D. A mixture of the carboxylic acid (3 eq.), *N*-methylimidazole (3.5 eq.) and chloro-*N,N,N',N'*-tetramethylformamidinium-hexafluorophosphate (1.2 eq.) were stirred in acetonitrile for 15 min. The amine (1 eq.) was dissolved in some acetonitrile then was added to the mixture. The formed reaction mixture was stirred at room temperature for 20 hr. After completion of the reaction was confirmed by TLC, water was added, and the mixture was extracted using ethyl acetate. The combined organic layer was washed with water followed by brine. After drying over anhydrous sodium sulfate, the organic layer was filtered then concentrated in vacuo to yield the crude compound which was purified using MPLC. The yield was around 67%.

Method IV, azide-alkyne Huisgen cycloaddition

In a two-necked flask, a mixture of azide containing conjugate (1 eq.), propagyl group containing ligand (1 eq.), sodium ascorbate (0.2 eq.) and copper(II) sulfate pentahydrate (0.2 eq.) was dissolved in a solvent mixture composed of tetrahydrofuran and water (2:1). After purging the reaction mixture with argon, the flask was placed in the dark and the mixture was stirred for 24h at room temperature. After the completion of the reaction, the solvent was evaporated under reduced pressure. The remaining residue was dissolved in 1M aqueous ammonium chloride, and the formed aqueous solution was extracted with ethyl acetate. The combined organic layer was washed with brine then it was dried over anhydrous sodium sulfate. Finally, the solvent was evaporated under reduced pressure to yield the crude product which was purified using the MPLC. The yield was around 67-70 %.

Method V, deprotection of tetrahydropyranyl ether

To a solution of the 2-tetrahydropyranyl-protected product (1 eq.) in tetrahydrofuran or tetrahydrofuran with few drops of methanol, 10-15 drops of 1M hydrochloric acid were added, and the reaction mixture was sonicated at 0°C or room temperature for 2h or until TLC showed completion of the reaction. The solvent was then evaporated under vacuum and the crude product was purified by preparative HPLC. The yields were around 20-50%.

Method VI, deprotection of tert-butyl protected carbamates and tert-butyl ester protected carboxylic acids

To a solution of tert-butyl protected carbamate (1 mmol) or tert-butyl ester protected carboxylic acid (1 mmol) in dichloromethane, trifluoroacetic acid (1 mL) was added. The reaction mixture was then stirred at room temperature for 2-24h. After completion of the reaction, the solvent and excess trifluoroacetic acid were evaporated under reduced pressure to yield the crude product which was purified using the MPLC. The yields were around 78-100%.

Method VII, catalytic hydrogenation

A mixture of the benzyl-protected starting material (1 eq.) was dissolved in tetrahydrofuran or ethyl acetate or methanol or a mixture of tetrahydrofuran and ethyl acetate (1:1) then a catalytic amount of 5% Pd/C catalyst was added. The reaction mixture was put under vacuum followed by hydrogen atmosphere. The mixture was stirred at room temperature until complete consumption of the starting material. The mixture was then filtered through celite, and the solvent was evaporated to give the crude residue which was purified using MPLC. The yields were around 25-90%.

3. *In vitro* HDAC inhibitory activity

HDAC1, HDAC6 and HDAC8

The *in vitro* testing on recombinant HDACs were performed as previously described [62] Recombinant human HDAC1 and -6 were purchased from BPS Biosciences. The enzyme inhibition was determined by using a reported homogenous fluorescence assay. [63] The enzymes were incubated for 90 min at 37°C, with the fluorogenic substrate ZMAL (Z-(Ac)Lys-AMC) in a concentration of 10.5 mM and increasing concentrations of inhibitors with subsequent addition of 60 mL of buffer containing trypsin (1 mg/ml) and TSA (2.75 mM) and further incubation for 20 min at 37°C. Fluorescence intensity was measured at an excitation wavelength of 390 nm and an emission wavelength of 460 nm in a microtiter plate reader (BMG Polarstar).

Recombinant hHDAC8 was produced by Romier et al. in Strasbourg. [64] The HDAC8 activity assays were performed according to the commercial HDAC8 Fluorometric Drug Discovery Kit [Fluor de Lys(R)-HDAC8, BML-KI178] corresponding to the manufacturer's instructions. As substrate a tetrapeptide connected to aminomethylcoumarin (AMC) H2N-Arg- His-Lys(Ac)-Lys(Ac)-AMC was synthesized as previously described. [62] The enzyme was incubated for 90 min at 37 °C, with a substrate concentration of 50 μM and increasing concentrations of inhibitors. The stop-solution containing inhibitor, to stop the hHDAC8 activity, and Trypsin, to release the AMC, was added. The solution was incubated for 20 min at 37 °C to develop the assay. Fluorescence intensity was measured at an excitation wavelength of 355 nm and an emission wavelength of 460 nm in a microtiter plate reader (BMG Polarstar).

Inhibition was measured at increasing concentration and IC_{50} was calculated by nonlinear regression with Origin 9.0G software.

4.   Cellular testing

A. Cell Culture

Human neuroblastoma cell lines SK-N-BE(2)-C (European Collection of Authenticated Cell Cultures, ECACC, Salisbury, UK) and IMR-32 (German Collection of Microorganisms and Cell Cultures, DSMZ, Darmstadt, Germany) were cultured under standard conditions in Dulbecco's Modified Eagles Medium (DMEM containing L-glutamine and 4.5 g/L glucose, Gibco Invitrogen cell culture, Invitrogen, Paisley, UK) supplemented with 10% fetal calf serum (FCS; Sigma, St. Louis, MO, USA) and 1% non-essential amino acids (NEAA; Invitrogen, Carlsbad, CA, USA). All cell lines were regularly checked for mycoplasma and multiple contaminations (Multiplexion, Heidelberg, Germany) and routinely verified using DNA fingerprinting authentication by Multiplexion.

B. Western blot

Western blot analysis was performed as described previously (Kolbinger et al.). The following antibodies were used: anti-HDAC8 (H-145) (polyclonal; Santa Cruz, Santa Cruz, CA, USA), anti-HDAC6 (sc-11420, Santa Cruz), anti-HDAC10 (H3413, Sigma), anti-tubulin (#2148, Cell Signaling Technology), anti-acetylated tubulin (#6793, Sigma-Aldrich), anti-acetylated SMC3 (kindly provided by Katsuhiko Shirahige, Institute for Molecular and Cellular Biosciences, University of Tokyo, Japan (Nishiyama et al. 2010)), anti-GAPDH (clone 6C5; Merck) and anti-β-actin (#5441, Sigma-Aldrich).

C. Cell viability assay (Trypan blue assay)

Adherent cells were detached using trypsin–EDTA (ThermoFisher Scientific) and pooled with corresponding supernatant, centrifuged and resuspended in 1 ml of cell culture medium. Cell viability (viable cell number, % viability, % dead cells) was measured by automated trypan blue staining using the Vi-Cell XR Cell Viability Analyzer (Beckman Coulter, Krefeld, Germany).

D. Colony formation assay

In six-well plates, 500 cells were seeded and treated as indicated. Viable colonies were stained after a minimum of 10 days with crystal violet. For quantification, the mean intensity of each well of the 8-bit binary picture was measured with ImageJ software (U. S. National Institutes of Health, Bethesda, MD, USA; http://imagej.nih.gov/ij/)

E. Cell differentiation assay

Adherent cells plated on 6-well plates were treated as indicated. For staining, cells were rinsed once with (PBS) and incubated with crystal violet staining solution (1% (w/v) in 70% EtOH) for 1 min. Subsequently, the staining solution was removed and cells were rinsed two to three times with autoclaved purified water and allowed to dry. All-trans retinoic acid (ATRA, Sigma-Aldrich, stock concentration 10 mM) was dissolved in ethanol (EtOH, Sigma-Aldrich).

F. Cytotoxicity Studies.

HEK293 cells (DSMZ Braunschweig, ACC305) were incubated at 37 °C in a humidified incubator with 5% CO_2 in Dulbecco's modified Eagle medium (DMEM) supplemented with 10% FCS and 5 mM glutamine. The cells were seeded out at 1.5

× 103 cells per well in a 96-well cell culture plate (TPP, Switzerland). All tested compounds were added immediately to the medium at 50 µM or increasing concentrations to determine IC50 values. After 24 h, Alamar Blue reagent (Invitrogen, CA) was added according to the manufacturer's instructions and incubated again for 21 h before the samples were analyzed. Detection of the viable cells which convert the resazurine of reagent into the high fluorescent resorufin was performed by using a FLUOstar OPTIMA microplate reader (BMG Labtec) with the following filter set: Ex 560 nm/Em 590 nm.

The measurements were performed in triplicate, and data are the mean with SD ≤ 12%. As a positive control daunorubicin was used, and an IC_{50} value of 12.55 ± 0.07 µM was obtained.

5. Characterization data of the final compounds

3-(4-(6-((2-(2,6-Dioxopiperidin-3-yl)-1,3-dioxoisoindolin-4-yl)amino)hexanamido)benzamido)-*N*-hydroxy-4-methoxybenzamide (1a)
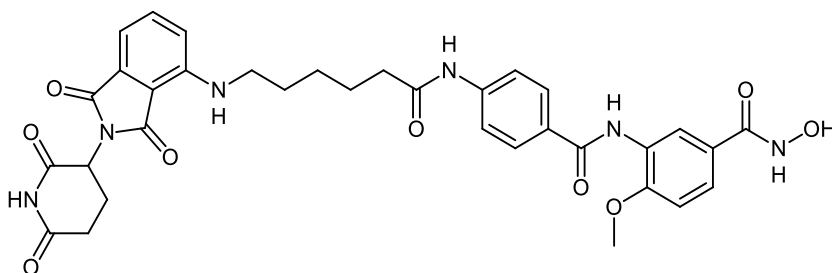
MS m/z: 669.34 [M-H]⁻

¹H NMR (400 MHz, DMSO-d6) δ 11.06 (s, 2H), 10.14 (s, 1H), 9.36 (s, 1H), 8.18 (d, *J* = 2.1 Hz, 1H), 7.90 (d, *J* = 8.8 Hz, 2H), 7.71 (d, *J* = 8.7 Hz, 2H), 7.62 – 7.52 (m, 2H), 7.12 (d, *J* = 8.7 Hz, 1H), 7.09 (d, *J* = 8.6 Hz, 1H), 7.00 (d, *J* = 7.0 Hz, 1H), 6.53 (t, *J* =

5.9 Hz, 1H), 5.03 (dd, J = 12.8, 5.4 Hz, 1H), 3.86 (s, 3H), 2.94 – 2.78 (m, 2H), 2.68 –

2.51 (m, 2H), 2.35 (t, J = 7.3 Hz, 2H), 2.09 – 1.90 (m, 2H), 1.63 (tt, J = 15.0, 7.3 Hz,

4H), 1.45 – 1.32 (m, 2H).

^{13}C NMR (101 MHz, DMSO-d6) δ 173.34, 172.28, 170.55, 169.38, 167.78, 165.05,

154.29, 146.87, 142.77, 136.79, 132.55, 128.86, 128.76, 127.04, 118.82, 118.53,

111.33, 110.89, 109.37, 56.47, 51.59, 49.03, 48.97, 36.81, 31.37, 28.91, 26.37,

25.17, 22.58.

HRMS: 693.227 [M+Na]$^+$, calculated $C_{34}H_{34}N_6O_9Na^+$: 693.228

HPLC: (M2) rt. 9.7 min (purity >99%)

3-(4-(8-((2-(2,6-Dioxopiperidin-3-yl)-1,3-dioxoisoindolin-4-

yl)amino)octanamido)benzamido)-*N*-hydroxy-4-methoxybenzamide (1b)

MS m/z: 697.62 [M-H]$^-$

^{1}H NMR (400 MHz, DMSO-d6) δ 11.05 (s, 2H), 10.14 (s, 1H), 9.36 (s, 1H), 8.17 (d, J

= 1.7 Hz, 1H), 7.90 (d, J = 8.7 Hz, 2H), 7.71 (d, J = 8.5 Hz, 2H), 7.64 – 7.49 (m, 2H),

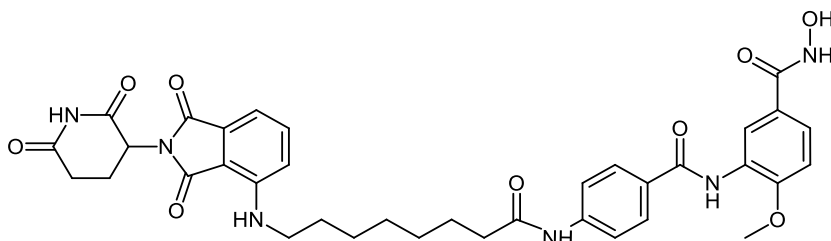7.12 (d, J = 8.7 Hz, 1H), 7.07 (d, J = 8.6 Hz, 1H), 7.00 (d, J = 7.0 Hz, 1H), 6.51 (t, J =

5.5 Hz, 1H), 5.03 (dd, J = 12.9, 5.2 Hz, 1H), 3.86 (s, 3H), 2.95 – 2.75 (m, 2H), 2.67 –

2.52 (m, 2H), 2.39 – 2.27 (m, 2H), 2.09 – 1.92 (m, 2H), 1.68 – 1.47 (m, 4H), 1.40 –

1.23 (m, 6H).

¹³C NMR (101 MHz, DMSO-d6) δ 173.25, 172.24, 170.52, 167.75, 164.94, 146.88, 142.84, 136.74, 132.61, 128.87, 118.74, 110.83, 109.43, 72.91, 63.51, 56.48, 48.99, 36.78, 31.41, 29.09, 29.04, 28.94, 26.63, 25.37.

HRMS: 699.279 [M+H]$^+$, calculated $C_{36}H_{39}N_6O_9^+$: 699.278

HPLC: (M2) rt. 10.3 min (purity 99%)

3-(4-(6-(2-(Adamantan-1-yl)acetamido)hexanamido)benzamido)-*N*-hydroxy-4-methoxybenzamide (1m)
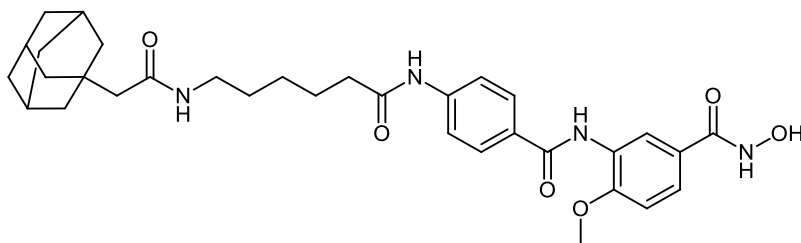
MS m/z: 589.45 [M-H]$^-$

¹H NMR (400 MHz, DMSO-d6) δ 11.05 (s, 2H), 10.14 (s, 1H), 9.36 (s, 1H), 8.18 (d, *J* = 2.1 Hz, 1H), 7.91 (d, *J* = 8.7 Hz, 2H), 7.71 (d, *J* = 8.7 Hz, 2H), 7.67 – 7.55 (m, 2H), 7.12 (d, *J* = 8.7 Hz, 1H), 3.87 (s, 3H), 3.00 (dd, *J* = 12.6, 6.6 Hz, 2H), 2.33 (t, *J* = 7.3 Hz, 2H), 1.94 – 1.84 (m, 3H), 1.79 (s, 2H), 1.69 – 1.47 (m, 14H), 1.46 – 1.35 (m, 2H), 1.35 – 1.24 (m, 2H).

¹³C NMR (101 MHz, DMSO-d6) δ 172.18, 170.29, 164.96, 154.26, 142.83, 128.84, 128.74, 127.10, 125.11, 124.86, 123.93, 118.76, 118.39, 111.31, 56.47, 50.54, 49.08, 39.23, 38.64, 36.90, 32.57, 29.42, 28.47, 26.58, 25.13.

HRMS: 591.319 [M+H]$^+$, calculated $C_{33}H_{43}N_4O_6^+$: 591.318

HPLC: (M2) rt. 10.5 min (purity 93 %)

3-(4-(8-(2-(Adamantan-1-yl)acetamido)octanamido)benzamido)-*N*-hydroxy-4-methoxybenzamide (1n)
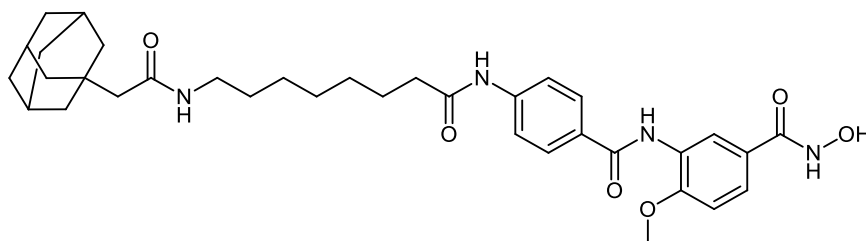

MS m/z: 617.60 [M-H]$^-$

^{1}H NMR (400 MHz, DMSO-d6) δ 11.02 (s, 2H), 10.13 (s, 1H), 9.35 (s, 1H), 8.17 (d, J = 2.1 Hz, 1H), 7.90 (d, J = 8.8 Hz, 2H), 7.71 (d, J = 8.8 Hz, 2H), 7.58 (dd, J = 8.5, 2.2 Hz, 2H), 7.11 (d, J = 8.7 Hz, 1H), 3.86 (s, 3H), 2.99 (dd, J = 12.6, 6.6 Hz, 2H), 2.32 (t, J = 7.4 Hz, 2H), 1.93 − 1.82 (m, 3H), 1.78 (s, 2H), 1.74 − 1.42 (m, 14H), 1.41 − 1.16 (m, 8H).

^{13}C NMR (101 MHz, DMSO-d6) δ 172.16, 170.09, 164.89, 154.19, 142.87, 128.85, 128.74, 127.14, 125.22, 124.88, 123.97, 118.71, 118.40, 111.28, 56.48, 50.56, 38.64, 36.92, 32.58, 29.61, 29.10, 28.95, 28.49, 26.77, 25.40.

HRMS: 619.350 [M+H]$^+$, calculated $C_{35}H_{47}N_4O_6^+$: 619.350

HPLC: (M2) rt. 14.2 min (purity > 99 %)

The synthesis of the PROTACs (**1a, 1b, 1m and 1n**) is elucidated in **scheme 1**. After 4-((tert-butoxycarbonyl) amino)benzoic acid (**4**) was prepared as previously reported [65], it was reacted with methyl 3-amino-4-methoxybenzoate (**6a**) following method IIIA to yield methyl 3-(4-((tert-butoxycarbonyl)amino)benzamido)-4-methoxybenzoate (**7**). Next, the methyl ester group was hydrolysed using the general method IIA and

the tert-butyloxycarbonyl protecting group was removed using method VI to yield 3-(4-aminobenzamido)-4-methoxybenzoic acid (**8**). To complete the synthesis of the 2-tetrahydropyranyl-protected HDAC ligand (**9**), *O*-(tetrahydro-2*H*-pyran-2-yl) hydroxylamine was reacted with the free carboxylic group following method IIIA. The 2-tetrahydropyranyl protected PROTACs were synthesised by reacting the different E3 ligase ligand-linker-COOH (**43a,b)** or HyT-linker-COOH (**47a,b**) (see synthesis in Supp. Info.) with the 2-tetrahydropyranyl-protected HDAC ligand (**9**) as stated in the general method IIIA. Finally, deprotection according to the general method V took place to obtain the free hydroxamic acid containing PROTACs (**1a, 1b, 1m and 1n).**

N^1-((*S*)-1-((2*S*,4*R*)-4-hydroxy-2-((4-(4-methylthiazol-5-yl)benzyl)carbamoyl)pyrrolidin-1-yl)-3,3-dimethyl-1-oxobutan-2-yl)-N^8-(4-((5-(hydroxycarbamoyl)-2-methoxyphenyl) carbamoyl) phenyl)octanediamide (1k)
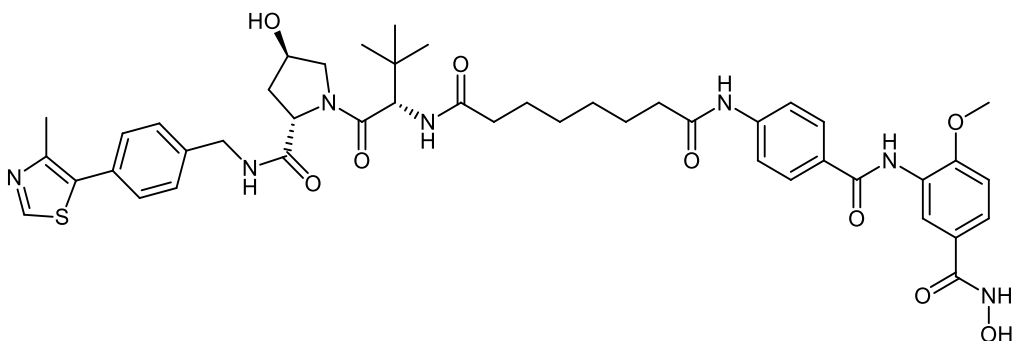
MS m/z: 868.41 [M-H]⁻

¹H NMR (400 MHz, DMSO-d6) δ 11.08 (s, 2H), 10.14 (s, 1H), 9.37 (s, 1H), 8.96 (s, 1H), 8.53 (t, *J* = 6.0 Hz, 1H), 8.17 (d, *J* = 2.1 Hz, 1H), 7.91 (d, *J* = 8.8 Hz, 2H), 7.82 (d, *J* = 9.3 Hz, 1H), 7.71 (d, *J* = 8.8 Hz, 2H), 7.59 (dd, *J* = 8.6, 2.2 Hz, 1H), 7.46 – 7.29 (m, 3H), 7.12 (d, *J* = 8.7 Hz, 1H), 5.11 (s, 1H), 4.53 (d, *J* = 9.4 Hz, 1H), 4.46 – 4.29 (m, 3H), 4.20 (dd, *J* = 15.9, 5.5 Hz, 1H), 3.86 (s, 3H), 3.70 – 3.52 (m, 2H), 2.43

(s, 3H), 2.29 – 1.94 (m, 4H), 1.64 – 1.39 (m, 4H), 1.34 – 1.20 (m, 4H), 0.92 (s, J = 7.9 Hz, 9H).

^{13}C NMR (101 MHz, DMSO-d6) δ 173.09, 172.69, 172.68, 172.43, 172.29, 170.17, 164.99, 154.27, 151.89, 148.13, 142.82, 139.88, 131.61, 130.05, 129.07, 128.86, 128.74, 127.86, 127.10, 127.08, 125.07, 118.78, 118.77, 118.52, 111.32, 69.31, 59.15, 56.80, 56.77, 56.47, 49.03, 38.33, 35.63, 35.32, 28.89, 28.84, 26.80, 25.77, 25.35, 16.33.

HRMS: 870.388 [M+H]$^+$, calculated $C_{45}H_{56}N_7O_9S^+$ 870.386

HPLC: (M2) rt. 9.9 min (purity 96%)

In **scheme 2**, the synthesis of PROTAC (**1k**) is shown. First, the 2-tetrahydropyranyl-protected HDAC ligand (**9**) was synthesized as previously indicated in **scheme 1**. Next, suberic acid was attached to the protected ligand following method IIID to yield 8-((4-((2-methoxy-5-(((tetrahydro-2*H*-pyran-2-yl)oxy)carbamoyl)phenyl)carbamoyl)phenyl)amino)-8-oxooctanoic acid (**10**). Then the formed conjugate was reacted with the VHL ligand **(40)** using method IIIA to give the protected PROTAC which was deprotected according to method V.

3-(4-((8-((2-(2,6-Dioxopiperidin-3-yl)-1,3-dioxoisoindolin-4-yl)amino)octanamido)methyl)benzamido)-*N*-hydroxy-4-methoxybenzamide (1c)
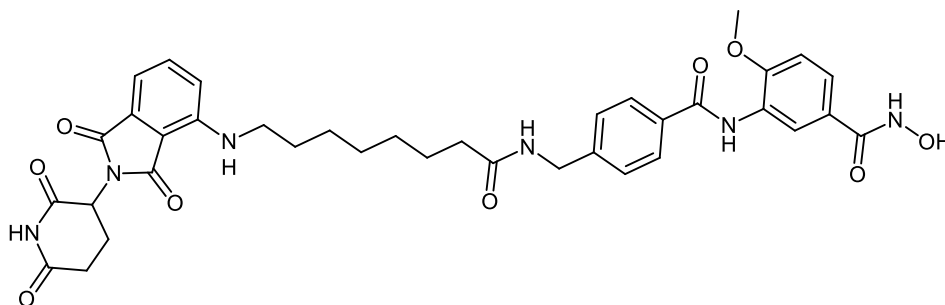
MS m/z: 711.36 [M-H] $^-$

^{1}H NMR (400 MHz, DMSO-d6) δ 11.04 (s, 2H), 9.45 (s, 1H), 8.35 (t, J = 5.9 Hz, 1H), 8.17 (d, J = 2.1 Hz, 1H), 7.90 (d, J = 8.2 Hz, 2H), 7.66 – 7.50 (m, 2H), 7.35 (d, J = 8.2 Hz, 2H), 7.12 (d, J = 8.7 Hz, 1H), 7.07 (d, J = 8.6 Hz, 1H), 6.99 (d, J = 7.0 Hz, 1H), 6.50 (t, J = 5.7 Hz, 1H), 5.02 (dd, J = 12.8, 5.4 Hz, 1H), 4.31 (d, J = 5.8 Hz, 2H), 3.85 (s, 3H), 3.00 – 2.73 (m, 2H), 2.69 – 2.51 (m, 2H), 2.14 (t, J = 7.4 Hz, 2H), 2.07 – 1.86 (m, 2H), 1.67 – 1.40 (m, 4H), 1.40 – 1.14 (m, 6H).

^{13}C NMR (101 MHz, DMSO-d6) δ 173.22, 172.71, 170.52, 169.39, 167.73, 165.30, 154.32, 146.87, 144.20, 136.71, 133.15, 132.63, 127.98, 127.54, 127.01, 125.17, 125.06, 124.14, 117.61, 111.34, 110.81, 109.46, 56.48, 49.04, 48.99, 42.27, 35.76, 31.42, 29.08, 28.92, 26.67, 25.68, 22.59.

HRMS: 713.295 [M+H] $^+$, calculated $C_{37}H_{41}N_6O_9^+$: 713.294

HPLC: (M2) rt. 12.2 min (purity >99 %)

3-(4-((8-(2-(Adamantan-1-yl)acetamido)octanamido)methyl)benzamido)-*N*-hydroxy-4-methoxybenzamide (**1o**)
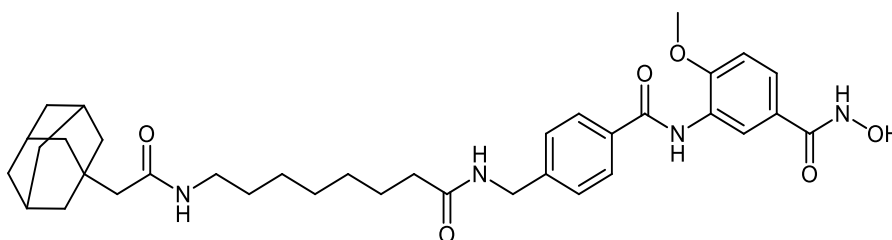

MS m/z: 631.54 [M-H]$^-$

^{1}H NMR (400 MHz, DMSO-d6) δ 10.82 (s, 2H), 9.45 (s, 1H), 8.36 (t, J = 5.9 Hz, 1H), 8.16 (d, J = 2.1 Hz, 1H), 7.90 (d, J = 8.3 Hz, 2H), 7.70 – 7.51 (m, 2H), 7.35 (d, J = 8.3

Hz, 2H), 7.12 (d, J = 8.7 Hz, 1H), 4.31 (d, J = 5.9 Hz, 2H), 3.85 (s, 3H), 2.99 (dd, J = 12.6, 6.7 Hz, 2H), 2.13 (t, J = 7.4 Hz, 2H), 1.94 – 1.83 (m, 3H), 1.78 (s, 2H), 1.73 – 1.42 (m, 12H), 1.43 – 1.30 (m, 2H), 1.29 – 1.12 (m,8H).

^{13}C NMR (101 MHz, DMSO-d6) δ 172.68, 170.10, 165.29, 154.31, 144.19, 133.16, 127.98, 127.76, 127.55, 127.51, 127.00, 125.27, 124.18, 111.33, 56.48, 50.54, 42.59, 36.92, 35.78, 32.58, 29.62, 29.13, 28.90, 28.49, 26.80, 25.68.

HRMS: 633.366 [M+H]$^+$, calculated $C_{36}H_{49}N_4O_6^+$: 633.365

HPLC: (M2) rt. 13.8 min (purity 99%)

According to the general method IIIB compound 3-(4-(((tert-butoxycarbonyl)amino)methyl) benzamido)-4-methoxybenzoic acid (**13**) was synthesized starting from 4-(((tert-butoxycarbonyl)amino)methyl)benzoic acid (**11**) and methyl 3-amino-4-methoxybenzoate (**6a**). Tert-butyl (4-(chlorocarbonyl) benzyl)carbamate (**12**) was prepared in accordance to a previously reported method [66]. The methyl ester was hydrolysed according to method IIA to obtain the free carboxylic acid which was reacted with *O*-benzylhydroxylamine hydrochloride according to method IIIA to give the benzyl protected HDAC ligand (**14**). Next, the tert-butyloxycarbonyl protecting group was removed using method VI. The PROTAC synthesis was completed by reacting the E3 ligase ligand-linker-COOH (**43b**) or HyT-linker-COOH (**47b**) with the protected HDAC ligand (**14**) using method IIIA followed by removing the benzyl group according to the method VII to obtain the free hydroxamic acid. The synthesis of the PROTACs (**1c** and **1o**) is shown in **scheme 3**.

3-((4-((1-(6-((2-(2,6-Dioxopiperidin-3-yl)-1,3-dioxoisoindolin-4-yl)amino)-6-oxohexyl)-1*H*-1,2,3-triazol-4-yl)methoxy)benzyl)amino)-*N*-hydroxy-4-methylbenzamide (1d)
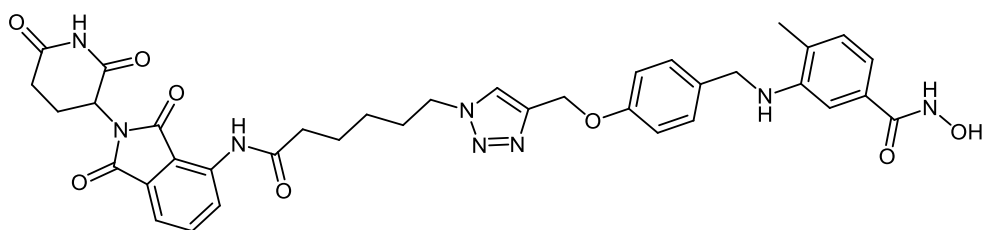
MS m/z: 721.67 [M-H]$^-$

^{1}H NMR (400 MHz, DMSO-d6) δ 11.11 (s, 1H), 10.88 (s, 1H), 9.67 (s, 1H), 8.75 (d, J = 1.7 Hz, 1H), 8.44 (d, J = 8.5 Hz, 1H), 8.18 (s, 1H), 7.83 – 7.77 (m, 1H), 7.59 (d, J = 7.2 Hz, 1H), 7.26 (d, J = 8.5 Hz, 2H), 7.00 – 6.92 (m, 3H), 6.86 – 6.80 (m, 2H), 5.61 (t, J = 5.9 Hz, 1H), 5.12 (dd, J = 12.7, 5.3 Hz, 1H), 5.06 (s, 2H), 4.38 – 4.27 (m, 4H), 2.92 – 2.81 (m, 1H), 2.63 – 2.51 (m, 2H), 2.45 – 2.41 (m, 1H), 2.14 (s, 3H), 1.89 – 1.78 (m, 2H), 1.69 – 1.58 (m, 2H), 1.57 – 1.46 (m, 2H), 1.33 – 1.26 (m, 2H).

^{13}C NMR (101 MHz, cd$_3$od) δ 172.46, 172.32, 169.06, 168.96, 166.88, 157.41, 146.20, 143.85, 137.12, 136.23, 131.91, 131.21, 130.44, 129.87, 128.76, 126.17, 125.23, 123.31, 118.50, 115.28, 114.91, 108.24, 77.50, 61.64, 50.09, 49.28, 37.12, 31.18, 29.72, 25.71, 24.29, 22.49, 17.23.

HRMS: 723.290 [M+H]$^+$, calculated C$_{37}$H$_{39}$N$_8$O$_8$$^+$ 723.289

HPLC: (M2) rt: 7.3 min (purity 96 %)

3-((4-((1-(6-((2-(2,6-Dioxopiperidin-3-yl)-1,3-dioxoisoindolin-4-yl)amino)-6-oxohexyl)-1*H*-1,2,3-triazol-4-yl)methoxy)benzyl)amino)-*N*-hydroxy-4-methoxybenzamide (1e)

MS m/z: 737.62 [M-H]⁻

^{1}H NMR (400 MHz, DMSO-d6) δ 11.10 (s, 1H), 10.87 (s, 1H), 9.67 (s, 1H), 8.72 (s, 4H), 8.44 (d, J = 8.4 Hz, 1H), 8.18 (s, 1H), 7.80 (t, J = 7.9 Hz, 1H), 7.59 (d, J = 7.3 Hz, 1H), 7.24 (d, J = 8.5 Hz, 2H), 6.98 (d, J = 1.6 Hz, 1H), 6.94 (d, J = 8.8 Hz, 2H), 6.86 (d, J = 1.3 Hz, 1H), 6.81 (d, J = 8.3 Hz, 1H), 5.48 (t, J = 6.0 Hz, 1H), 5.12 (dd, J = 12.7, 5.4 Hz, 1H), 5.06 (s, 2H), 4.34 (t, J = 7.1 Hz, 2H), 4.26 (d, J = 6.1 Hz, 2H), 3.81 (s, 3H), 2.67 – 2.51 (m, 2H), 2.46 – 2.34 (m, 2H), 2.13 – 2.00 (m, 1H), 1.91 – 1.78 (m, 2H), 1.70 – 1.58 (m, 2H), 1.53 – 1.40 (m, 1H), 1.37 – 1.25 (m, 2H).

^{13}C NMR (101 MHz, DMSO-d6) δ 173.17, 172.30, 170.20, 168.08, 167.09, 157.38, 149.04, 143.13, 137.88, 136.94, 136.51, 132.64, 131.90, 128.72, 126.78, 125.74, 124.73, 118.75, 117.48, 114.97, 109.33, 61.61, 55.99, 49.66, 49.36, 45.93, 36.62, 31.37, 29.85, 25.78, 24.55, 22.43.

HRMS: 739.284 [M+H]⁺, calculated $C_{37}H_{39}N_8O_9^+$ 739.284

HPLC: (M2) rt: 10.9 min (purity 99 %)

4-Chloro-3-((4-((1-(6-((2-(2,6-dioxopiperidin-3-yl)-1,3-dioxoisoindolin-4-yl)amino)-6-oxohexyl)-1*H*-1,2,3-triazol-4-yl)methoxy)benzyl)amino)-*N*-hydroxybenzamide (1f)

MS m/z: 741.59 [M-H]$^-$

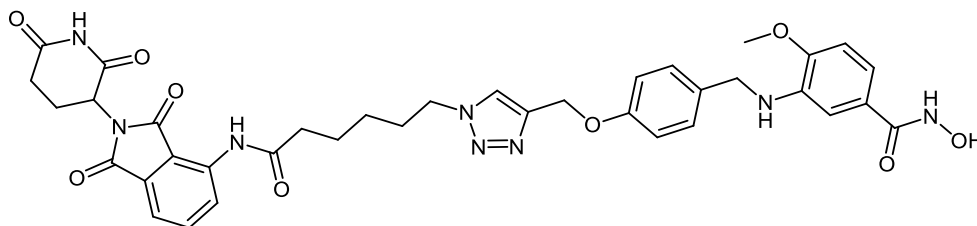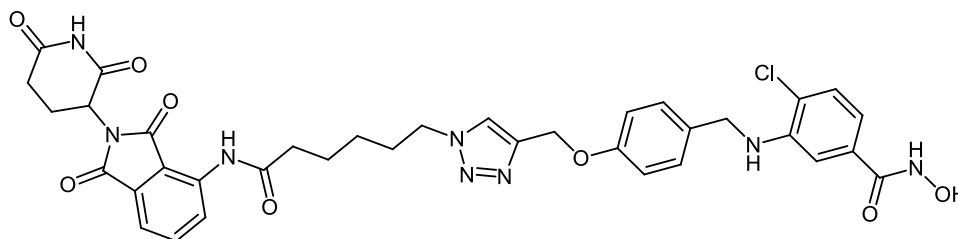^{1}H NMR (400 MHz, DMSO-d6) δ 11.11 (s, 2H), 9.67 (s, 1H), 8.94 (s, 1H), 8.44 (d, J = 8.4 Hz, 1H), 8.18 (s, 1H), 7.84 − 7.75 (m, 1H), 7.58 (d, J = 7.2 Hz, 1H), 7.32 − 7.21 (m, 3H), 7.00 − 6.93 (m, 3H), 6.90 (dd, J = 8.2, 1.8 Hz, 1H), 6.13 (t, J = 5.9 Hz, 1H), 5.12 (dd, J = 12.8, 5.4 Hz, 1H), 5.06 (s, 2H), 4.41 − 4.29 (m, 4H), 2.65 − 2.50 (m, 2H), 2.47 − 2.37 (m, 2H), 2.30 − 2.20 (m, 1H), 1.90 − 1.75 (m, 2H), 1.70 − 1.59 (m, 2H), 1.56 − 1.46 (m, 1H), 1.36 − 1.24 (m, 2H).

^{13}C NMR (101 MHz, DMSO-d6) δ 173.17, 172.30, 170.20, 168.09, 167.09, 157.44, 144.23, 143.10, 136.94, 136.51, 132.82, 132.00, 131.90, 129.25, 128.49, 126.79, 124.74, 120.84, 118.75, 117.48, 115.05, 110.31, 61.60, 49.66, 49.36, 45.70, 36.63, 31.37, 29.85, 25.79, 24.55, 22.44.

HRMS: 743.235 [M+H]$^+$, calculated C$_{36}$H$_{36}$ClN$_8$O$_8$$^+$ 743.234

HPLC: (M1) rt: 12.9 min (purity 97 %)

To prepare 4-substituted-3-{[4-(proparg-1-yloxy)benzyl]amino}benzoic acid (**17a-c**), 4-proparg-1-yloxybenzaldehyde (**16**) and the corresponding amine **(5 a-c)** were

reacted according to the method IA. Afterwards, the 2-tetrahydropyranyl-protected HDAC ligand were prepared by reacting the free carboxylic acid in (**17a-c**) with *O*-(tetrahydro-2*H*-pyran-2-yl)hydroxylamine following the general method IIIA. Next, these HDAC ligands (**18a-c**) were linked to the E3 ligase ligand–linker-N_3 (**50**) via the azide-alkyne Huisgen cycloaddition as stated in method IV. Finally, the free hydroxamic acid was obtained by removing the 2-tetrahydropyranyl group following method V. The synthesis of these PROTACs (**1d-f**) is presented in **scheme 4**.

4-Chloro-3-[(4-{2-[(5-{[2-(2,6-dioxopiperidin-3-yl)-1,3-dioxoisoindolin-4-yl]amino}pentyl)amino]-2-oxoethoxy}benzyl)amino]-*N*-hydroxybenzamide (1g)
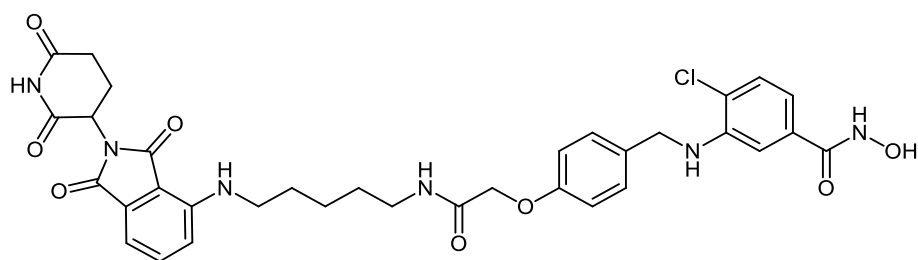
MS m/z: 689.24 [M-H]⁻

^{1}H NMR (400 MHz, DMSO-d^6) δ 11.06 (s, 2H), 8.93 (s, 1H), 8.01 (t, J = 5.7 Hz, 1H), 7.59 – 7.51 (m, 1H), 7.31 – 7.19 (m, 3H), 7.06 (d, J = 8.6 Hz, 1H), 7.00 (d, J = 7.0 Hz, 1H), 6.96 – 6.83 (m, 4H), 6.49 (t, J = 5.7 Hz, 1H), 6.14 (t, J = 6.1 Hz, 1H), 5.03 (dd, J = 12.9, 5.3 Hz, 1H), 4.40 (s, 2H), 4.35 (d, J = 6.0 Hz, 2H), 3.25 (dd, J = 13.5, 6.8 Hz, 2H), 3.11 (dd, J = 13.0, 6.6 Hz, 2H), 2.92 – 2.79 (m, 1H), 2.60 – 2.52 (m, 2H), 2.04 – 1.96 (m, 1H), 1.58 – 1.40 (m, 4H), 1.34 – 1.24 (m, 2H).

^{13}C NMR (101 MHz, DMSO-d^6) δ 173.21, 170.51, 169.38, 167.91, 167.73, 164.34, 157.10, 146.85, 144.21, 136.71, 132.81, 132.63, 132.37, 129.25, 128.42, 120.85,

117.61, 115.21, 115.11, 110.83, 110.29, 109.48, 79.61, 67.53, 49.00, 45.70, 42.24, 38.56, 31.43, 30.83, 29.21, 28.78, 24.06, 22.61.

HRMS m/z: 691.229 [M+H]$^+$, calculated C$_{34}$H$_{36}$ClN$_6$O$_8$$^+$: 691.228

HPLC: (M2) rt 9.5 min (purity 98 %)

4-Chloro-3-({4-[(16-{[2-(2,6-dioxopiperidin-3-yl)-1,3-dioxoisoindolin-4-yl]amino}-2-oxo-7,10,13-trioxa-3-azahexadecyl)oxy]benzyl}amino)-*N*-hydroxybenzamide (1h)
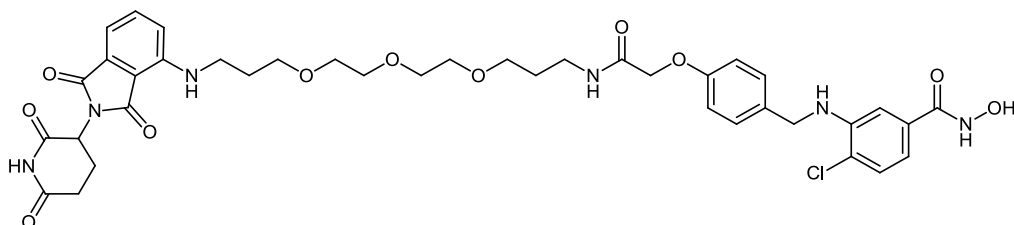
MS m/z: 807.53 [M-H]$^-$

^{1}H NMR (400 MHz, DMSO-d^6) δ 11.05 (s, 2H), 8.92 (s, 1H), 7.97 (t, J = 5.7 Hz, 1H), 7.55 (dd, J = 8.4, 7.2 Hz, 1H), 7.30 – 7.20 (m, 3H), 7.07 (d, J = 8.6 Hz, 1H), 6.99 (d, J = 6.9 Hz, 1H), 6.94 (d, J = 1.9 Hz, 1H), 6.91 – 6.85 (m, 3H), 6.63 (t, J = 5.9 Hz, 1H), 6.14 (t, J = 6.1 Hz, 1H), 5.02 (dd, J = 12.8, 5.4 Hz, 1H), 4.39 (s, 2H), 4.35 (d, J = 6.1 Hz, 2H), 3.55 – 3.39 (m, 10H), 3.40 – 3.29 (m, 4H), 3.14 (dd, J = 12.9, 6.7 Hz, 2H), 2.92 – 2.79 (m, 1H), 2.66 – 2.52 (m, 2H), 2.04 – 1.95 (m, 1H), 1.82 – 1.73 (m, 2H), 1.67 – 1.56 (m, 2H).

^{13}C NMR (101 MHz, DMSO-d^6) δ 173.22, 170.50, 169.27, 167.84, 167.77, 157.06, 146.88, 144.21, 136.70, 132.83, 132.64, 132.40, 129.25, 128.42, 117.52, 115.22, 115.15, 110.81, 110.28, 110.52, 70.22, 70.17, 70.13, 69.99, 68.65, 67.52, 48.98, 45.69, 36.30, 31.42, 29.69, 29.32, 22.61.

HRMS m/z: 809.292 [M+H]$^+$, calculated $C_{39}H_{46}ClN_6O_{11}^+$ 809.291

HPLC: (M2) rt 9.8 min (purity >99 %)

(2*S*,4*R*)-1-[(*S*)-2-(6-{2-[4-({[2-chloro-5-(hydroxycarbamoyl)phenyl] amino}methyl) phenoxy]acetamido}hexanamido)-3,3-dimethylbutanoyl]-4-hydroxy-*N*-[4-(4-methylthiazol-5-yl)benzyl]pyrrolidine-2-carboxamide (1l)
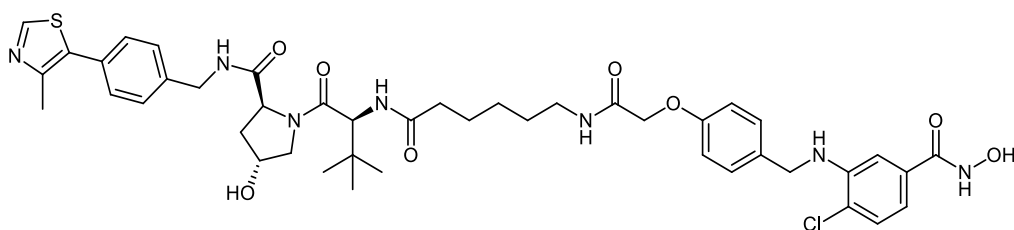
MS m/z: 874.38 [M-H]$^-$

^{1}H NMR (400 MHz, DMSO-d^6) δ 11.06 (s, 1H), 9.00 (s, 1H), 8.54 (t, J = 6.0 Hz, 1H), 7.99 (t, J = 5.8 Hz, 1H), 7.81 (d, J = 9.4 Hz, 1H), 7.43 − 7.33 (m, 4H), 7.30 − 7.20 (m, 3H), 6.96 − 6.85 (m, 4H), 4.52 (d, J = 9.3 Hz, 1H), 4.43 − 4.29 (m, 6H), 3.69 − 3.52 (m, 3H), 3.07 (dd, J = 13.2, 6.7 Hz, 2H), 2.43 (s, 3H), 2.26 − 2.16 (m, 1H), 2.11 − 1.98 (m, 2H), 1.93 − 1.83 (m, 1H), 1.77 − 1.71 (m, 1H), 1.52 − 1.32 (m, 4H), 1.25 − 1.15 (m, 3H), 0.91 (s, 9H).

^{13}C NMR (101 MHz, DMSO-d^6) δ 172.48, 172.37, 170.14, 167.83, 164.28, 157.10, 152.05, 147.87, 144.20, 140.02, 132.36, 129.94, 129.25, 129.08, 128.41, 127.87, 120.84, 115.24, 115.11, 110.31, 79.63, 69.30, 67.51, 59.13, 56.74, 38.63, 38.39, 35.65, 35.29, 29.29, 26.83, 26.50, 25.61, 16.26.

HRMS m/z: 876.353 [M+H] $^+$, calculated $C_{44}H_{55}ClN_7O_8S^+$: 876.352

HPLC: (M2) rt. 10.2 min (purity 96%)

3-({4-[2-({5-[2-(Adamantan-1-yl)acetamido]pentyl}amino)-2-oxoethoxy]benzyl}amino)-4-chloro-*N*-hydroxybenzamide (1p)
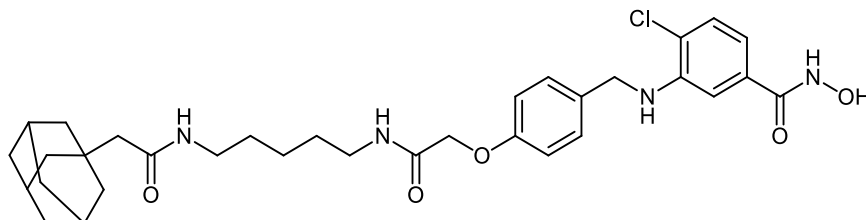
MS m/z: 609.65 [M-H]⁻

^{1}H NMR (400 MHz, DMSO-d^{6}) δ 11.05 (s, 1H), 8.91 (s, 1H), 7.98 (t, J = 5.8 Hz, 1H), 7.59 (s, 1H), 7.30 – 7.21 (m, 3H), 6.96 – 6.84 (m, 4H), 6.15 (t, J = 6.0 Hz, 1H), 4.39 (s, 2H), 4.36 (d, J = 6.1 Hz, 2H), 3.15 (d, J = 5.3 Hz, 1H), 3.08 (dd, J = 13.1, 6.6 Hz, 2H), 2.96 (dd, J = 12.8, 6.7 Hz, 2H), 1.88 (s, 3H), 1.78 (s, 2H), 1.66 – 1.49 (m, 11H), 1.42 – 1.30 (m, 4H), 1.25 – 1.15 (m, 2H).

^{13}C NMR (101 MHz, DMSO-d^{6}) δ 170.13, 167.85, 164.35, 157.10, 144.23, 132.83, 132.37, 129.25, 128.40, 115.22, 115.15, 110.29, 67.53, 50.51, 45.69, 42.59, 39.36, 38.65, 36.92, 32.58, 29.30, 29.20, 28.49, 24.22.

HRMS m/z: 611.300 [M+H]⁺, calculated C$_{33}$H$_{44}$ClN$_4$O$_5$⁺ : 611.300

HPLC: (M2) rt. 11 min (purity 98 %)

Benzyl 2-(4-(((2-chloro-5-(((tetrahydro-2*H*-pyran-2-yl)oxy)carbamoyl) phenyl) amino) methyl) phenoxy) acetate (**19**) was synthesized as shown in **scheme S1.2** in Supp. Info. Afterwards the benzyl protecting group was removed according to method VII to yield the 2-tetrahydropyranyl protected HDAC ligand (**20**), which was reacted with E3 ligase-linker-NH$_2$ conjugates (**53, 56, 59**) or HyT-linker-NH$_2$ (**57**) via method IIIA.

Finally, the protected PROTACs were deprotected using method V to yield PROTACs (**1g, 1h, 1l and 1p**) shown in **scheme 5**.

4-Chloro-3-(4-[(16-{[2-(2,6-dioxopiperidin-3-yl)-1,3-dioxoisoindolin-4-yl]amino}-2-oxo-7,10,13-trioxa-3-azahexadecyl)oxy]benzamido}-*N*-hydroxybenzamide (1i)
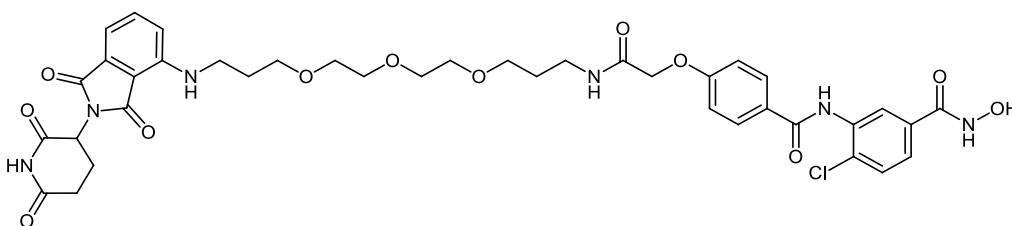

MS m/z: 821.47 [M-H]$^-$

^{1}H NMR (400 MHz, DMSO-d^6) δ 11.28 (s, 1H), 11.05 (s, 1H), 9.99 (s, 1H), 9.11 (s, 1H), 8.09 (t, J = 5.6 Hz, 1H), 7.99 – 7.93 (m, 3H), 7.66 – 7.49 (m, 3H), 7.13 – 6.96 (m, 4H), 6.64 (t, J = 5.8 Hz, 1H), 5.02 (dd, J = 12.8, 5.4 Hz, 1H), 4.55 (s, 2H), 3.57 – 3.29 (m, 14H), 3.17 (dd, J = 12.8, 6.7 Hz, 2H), 2.92 – 2.79 (m, 1H), 2.61 – 2.49 (m, 2H), 2.05 – 1.95 (m, 1H), 1.83 – 1.73 (m, 2H), 1.69 – 1.59 (m, 2H).

^{13}C NMR (101 MHz, DMSO-d^6) δ 173.22, 170.50, 169.29, 167.76, 167.51, 165.21, 161.05, 146.89, 136.70, 135.82, 132.63, 132.40, 130.04, 127.38, 126.40, 125.80, 117.53, 114.95, 110.82, 109.52, 70.24, 70.18, 70.14, 70.01, 68.63, 67.47, 48.98, 36.33, 31.42, 29.71, 29.33, 22.61.

HRMS m/z: 823.271 [M+H]$^+$, calculated $C_{39}H_{44}ClN_6O_{12}^+$: 823.271

HPLC: (M2) rt. 9.1 min (purity 99%)

The two starting materials 4-(2-methoxy-2-oxoethoxy)benzoic acid (**21**) [67] and benzyl 3-amino-4-chlorobenzoate (**22**) which were prepared as previously described

[68], were reacted together using method IIIC to afford benzyl 4-chloro-3-[4-(2-methoxy-2-oxoethoxy)benzamido]benzoate (**23**). Deprotection of the benzyl ester was achieved using method V, and the resulted acid was reacted with *O*-benzylhydroxylamine hydrochloride using method IIIA to afford methyl 2-[4-({5-[(benzyloxy)carbamoyl]-2-chlorophenyl}carbamoyl)phenoxy]acetate (**25**). The ester was then hydrolyzed using method IIB to afford the benzyl protected HDAC ligand 2-[4-({5-[(benzyloxy)carbamoyl]-2-chlorophenyl}carbamoyl)phenoxy]acetic acid (**26**). Finally, the protected HDAC ligand was reacted with E3 ligase-linker-NH$_2$ conjugate (**53**) following method IIIA to yield the protected PROTAC which was deprotected to yield PROTAC (**1i**) using method VII. **Scheme 6** illustrates the synthesis of the prescribed compound.

3-{4-[(16-{[2-(2,6-Dioxopiperidin-3-yl)-1,3-dioxoisoindolin-4-yl]amino}-2-oxo-7,10,13-trioxa-3-azahexadecyl)oxy]benzamido}-*N*-hydroxybenzamide (1j)
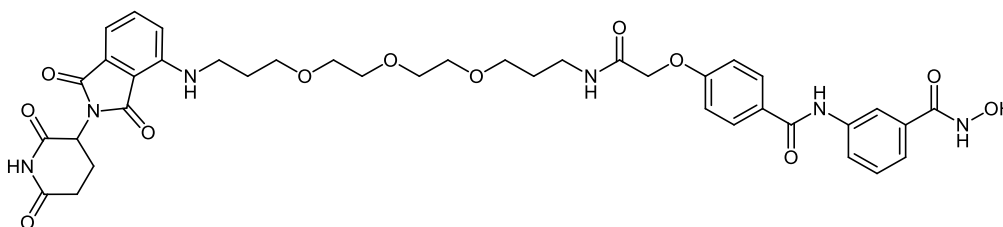
MS m/z: 787.37 [M-H]⁻

^{1}H NMR (400 MHz, DMSO-d^6) δ 11.16 (s, 1H), 11.06 (s, 1H), 10.21 (s, 1H), 8.99 (s, 1H), 8.16 (s, 1H), 8.09 (t, *J* = 5.5 Hz, 1H), 7.99 – 7.89 (m, 3H), 7.59 – 7.51 (m, 1H), 7.44 – 7.33 (m, 2H), 7.10 – 7.04 (m, 3H), 7.00 (d, *J* = 7.1 Hz, 1H), 6.64 (t, *J* = 5.7 Hz, 1H), 5.02 (dd, *J* = 12.8, 5.5 Hz, 1H), 4.55 (s, 2H), 3.56 – 3.29 (m, 14H), 3.19 – 3.13 (m, 2H), 2.86 – 2.78 (m, 1H), 2.67 – 2.50 (m, 2H), 2.05 – 1.93 (m, 1H), 1.83 – 1.74 (m, 2H), 1.68 – 1.59 (m, 2H).

HRMS m/z: 789.310 [M+H]$^+$, calculated $C_{39}H_{45}N_6O_{12}^+$: 789.310

HPLC: (M2) rt 8.7 min (purity 100%)

As illustrated in **scheme 6**, the use of 10% Pd/C in the catalytic hydrogenation to deprotect compound (**26**) resulted in the loss of the chlor in the final PROTAC (**1j**). That is the reason why a lower concentration of the catalyst was used. This led to the successful removal of the benzyl group while retaining the chlor atom.

Conflict of interest

None

Funding

Author Contributions

S.D and E.G synthesized some of the compounds and wrote parts of the manuscript. T. H. synthesized some of the compounds. D.H. and P.Z. carried out the HDAC in vitro testing and analysed data. D.R. did the docking and modelling studies. F.E. carried out the cytotoxicity testing on human HEK293 cells. R.S.-A. and J.R. performed experiments on neuroblastoma cells, C.R. expressed and provided HDAC8 protein for in vitro testing. M.S. carried out characterization of the final

compounds. M.J., I.O., and W.S. designed experiments, analysed data, and wrote the paper. All authors have given approval to the final version of the manuscript.

Supporting Information

This material is available free of charge. The Supporting Information is available free of charge on

Author Information

Corresponding Author

*Phone: +493455525040. E-mail: wolfgang.sippl@pharmazie.uni-halle.de

ORCID

Salma Darwish: 0000-0002-1782-356X

Manfred Jung: 0000-0002-6361-7716

Wolfgang Sippl: 0000-0002-5985-9261

References

1. Wolfson NA, Pitcairn CA, Fierke CA (2013) HDAC8 substrates: Histones and beyond. Biopolymers 99 (2):112-126. doi:https://doi.org/10.1002/bip.22135

2. Furdas SD, Kannan S, Sippl W, Jung M (2012) Small Molecule Inhibitors of Histone Acetyltransferases as Epigenetic Tools and Drug Candidates. Archiv der Pharmazie 345 (1):7-21. doi:https://doi.org/10.1002/ardp.201100209

3. Seto E, Yoshida M (2014) Erasers of histone acetylation: the histone deacetylase enzymes. Cold Spring Harb Perspect Biol 6 (4):a018713. doi:10.1101/cshperspect.a018713

4. Matthay KK, Maris JM, Schleiermacher G, Nakagawara A, Mackall CL, Diller L, Weiss WA (2016) Neuroblastoma. Nature Reviews Disease Primers 2 (1):16078. doi:10.1038/nrdp.2016.78

5. Oehme I, Deubzer HE, Wegener D, Pickert D, Linke JP, Hero B, Kopp-Schneider A, Westermann F, Ulrich SM, von Deimling A, Fischer M, Witt O (2009) Histone deacetylase 8 in neuroblastoma tumorigenesis. Clin Cancer Res 15 (1):91-99. doi:10.1158/1078-0432.Ccr-08-0684

6. Rettig I, Koeneke E, Trippel F, Mueller WC, Burhenne J, Kopp-Schneider A, Fabian J, Schober A, Fernekorn U, von Deimling A, Deubzer HE, Milde T, Witt O, Oehme I (2015) Selective inhibition of HDAC8 decreases neuroblastoma growth in vitro and in vivo and enhances retinoic acid-mediated differentiation. Cell Death Dis 6 (2):e1657-e1657. doi:10.1038/cddis.2015.24

7. Balasubramanian S, Ramos J, Luo W, Sirisawad M, Verner E, Buggy JJ (2008) A novel histone deacetylase 8 (HDAC8)-specific inhibitor PCI-34051 induces apoptosis in T-cell lymphomas. Leukemia 22 (5):1026-1034. doi:10.1038/leu.2008.9

8. Krennhrubec K, Marshall BL, Hedglin M, Verdin E, Ulrich SM (2007) Design and evaluation of 'Linkerless' hydroxamic acids as selective HDAC8 inhibitors. Bioorg Med Chem Lett 17 (10):2874-2878. doi:10.1016/j.bmcl.2007.02.064

9. Suzuki T, Ota Y, Ri M, Bando M, Gotoh A, Itoh Y, Tsumoto H, Tatum PR, Mizukami T, Nakagawa H, Iida S, Ueda R, Shirahige K, Miyata N (2012) Rapid discovery of highly potent and selective inhibitors of histone deacetylase 8 using click chemistry to generate candidate libraries. J Med Chem 55 (22):9562-9575. doi:10.1021/jm300837y

10. Suzuki T, Muto N, Bando M, Itoh Y, Masaki A, Ri M, Ota Y, Nakagawa H, Iida S, Shirahige K, Miyata N (2014) Design, synthesis, and biological activity of NCC149 derivatives as histone deacetylase 8-selective inhibitors. ChemMedChem 9 (3):657-664. doi:10.1002/cmdc.201300414

11. Huang WJ, Wang YC, Chao SW, Yang CY, Chen LC, Lin MH, Hou WC, Chen MY, Lee TL, Yang P, Chang CI (2012) Synthesis and biological evaluation of ortho-aryl N-hydroxycinnamides as potent histone deacetylase (HDAC) 8 isoform-selective inhibitors. ChemMedChem 7 (10):1815-1824. doi:10.1002/cmdc.201200300

12. Tang W, Luo T, Greenberg EF, Bradner JE, Schreiber SL (2011) Discovery of histone deacetylase 8 selective inhibitors. Bioorg Med Chem Lett 21 (9):2601-2605. doi:10.1016/j.bmcl.2011.01.134

13. Ingham OJ, Paranal RM, Smith WB, Escobar RA, Yueh H, Snyder T, Porco JA, Jr., Bradner JE, Beeler AB (2016) Development of a Potent and Selective HDAC8 Inhibitor. ACS Med Chem Lett 7 (10):929-932. doi:10.1021/acsmedchemlett.6b00239

14. Zhao G, Wang G, Bai H, Li T, Gong F, Yang H, Wen J, Wang W (2017) Targeted inhibition of HDAC8 increases the doxorubicin sensitivity of neuroblastoma cells via up regulation of miR-137. Eur J Pharmacol 802:20-26. doi:10.1016/j.ejphar.2017.02.035

15. Whitehead L, Dobler MR, Radetich B, Zhu Y, Atadja PW, Claiborne T, Grob JE, McRiner A, Pancost MR, Patnaik A, Shao W, Shultz M, Tichkule R, Tommasi RA, Vash B, Wang P, Stams T (2011) Human HDAC isoform selectivity achieved via exploitation of the acetate release channel with structurally unique small molecule inhibitors. Bioorg Med Chem 19 (15):4626-4634. doi:10.1016/j.bmc.2011.06.030

16. Heimburg T, Kolbinger FR, Zeyen P, Ghazy E, Herp D, Schmidtkunz K, Melesina J, Shaik TB, Erdmann F, Schmidt M, Romier C, Robaa D, Witt O, Oehme I, Jung M, Sippl W (2017) Structure-Based Design and Biological Characterization of Selective Histone Deacetylase 8 (HDAC8) Inhibitors with Anti-Neuroblastoma Activity. Journal of Medicinal Chemistry 60 (24):10188-10204. doi:10.1021/acs.jmedchem.7b01447

17. Lai AC, Crews CM (2017) Induced protein degradation: an emerging drug discovery paradigm. Nature Reviews Drug Discovery 16 (2):101-114. doi:10.1038/nrd.2016.211

18. Cromm PM, Crews CM (2017) Targeted Protein Degradation: from Chemical Biology to Drug Discovery. Cell Chemical Biology 24 (9):1181-1190.
doi:https://doi.org/10.1016/j.chembiol.2017.05.024

19. Itoh Y (2018) Chemical Protein Degradation Approach and its Application to Epigenetic Targets. The Chemical Record 18 (12):1681-1700. doi:https://doi.org/10.1002/tcr.201800032

20. Cecchini C, Pannilunghi S, Tardy S, Scapozza L (2021) From Conception to Development: Investigating PROTACs Features for Improved Cell Permeability and Successful Protein Degradation. Frontiers in Chemistry 9

21. Yin L, Hu Q (2020) Chimera induced protein degradation: PROTACs and beyond. European Journal of Medicinal Chemistry 206:112494. doi:https://doi.org/10.1016/j.ejmech.2020.112494

22. Schapira M, Calabrese MF, Bullock AN, Crews CM (2019) Targeted protein degradation: expanding the toolbox. Nature Reviews Drug Discovery 18 (12):949-963. doi:10.1038/s41573-019-0047-y

23. Ward CC, Kleinman JI, Brittain SM, Lee PS, Chung CYS, Kim K, Petri Y, Thomas JR, Tallarico JA, McKenna JM, Schirle M, Nomura DK (2019) Covalent Ligand Screening Uncovers a RNF4 E3 Ligase Recruiter for Targeted Protein Degradation Applications. ACS Chem Biol 14 (11):2430-2440. doi:10.1021/acschembio.8b01083

24. Zhang X, Crowley VM, Wucherpfennig TG, Dix MM, Cravatt BF (2019) Electrophilic PROTACs that degrade nuclear proteins by engaging DCAF16. Nature chemical biology 15 (7):737-746. doi:10.1038/s41589-019-0279-5

25. Bingqi Tong ML, Yi Xie ,Jessica Spradlin ,John A. Tallarico ,Jeffrey M. McKenna ,Markus Schirle ,Thomas J. Maimone ,Daniel Nomura (2020) Targeted Protein Degradation via a Covalent Reversible Degrader Based on Bardoxolone. ChemRxiv. doi:10.26434/chemrxiv.12055935.v1

26. Tong B, Luo M, Xie Y, Spradlin JN, Tallarico JA, McKenna JM, Schirle M, Maimone TJ, Nomura DK (2020) Bardoxolone conjugation enables targeted protein degradation of BRD4. Scientific Reports 10 (1):15543. doi:10.1038/s41598-020-72491-9

27. Burslem GM, Schultz AR, Bondeson DP, Eide CA, Savage Stevens SL, Druker BJ, Crews CM (2019) Targeting BCR-ABL1 in Chronic Myeloid Leukemia by PROTAC-Mediated Targeted Protein Degradation. Cancer Research 79 (18):4744-4753. doi:10.1158/0008-5472.CAN-19-1236

28. Schiedel M, Herp D, Hammelmann S, Swyter S, Lehotzky A, Robaa D, Oláh J, Ovádi J, Sippl W, Jung M (2018) Chemically Induced Degradation of Sirtuin 2 (Sirt2) by a Proteolysis Targeting Chimera (PROTAC) Based on Sirtuin Rearranging Ligands (SirReals). Journal of Medicinal Chemistry 61 (2):482-491. doi:10.1021/acs.jmedchem.6b01872

29. Xue G, Chen J, Liu L, Zhou D, Zuo Y, Fu T, Pan Z (2020) Protein degradation through covalent inhibitor-based PROTACs. Chemical Communications 56 (10):1521-1524. doi:10.1039/C9CC08238G

30. Gabizon R, Shraga A, Gehrtz P, Livnah E, Shorer Y, Gurwicz N, Avram L, Unger T, Aharoni H, Albeck S, Brandis A, Shulman Z, Katz B-Z, Herishanu Y, London N (2020) Efficient Targeted Degradation via Reversible and Irreversible Covalent PROTACs. Journal of the American Chemical Society 142 (27):11734-11742. doi:10.1021/jacs.9b13907

31. Neklesa T, Snyder LB, Willard RR, Vitale N, Raina K, Pizzano J, Gordon D, Bookbinder M, Macaluso J, Dong H, Liu Z, Ferraro C, Wang G, Wang J, Crews CM, Houston J, Crew AP, Taylor I (2018) Abstract 5236: ARV-110: An androgen receptor PROTAC degrader for prostate cancer. Cancer Research 78 (13_Supplement):5236-5236. doi:10.1158/1538-7445.AM2018-5236

32. Flanagan JJ, Qian Y, Gough SM, Andreoli M, Bookbinder M, Cadelina G, Bradley J, Rousseau E, Willard R, Pizzano J, Crews CM, Crew AP, Taylor I, Houston J (2019) Abstract P5-04-18: ARV-471, an oral estrogen receptor PROTAC degrader for breast cancer. Cancer Research 79 (4_Supplement):P5-04-18-P05-04-18. doi:10.1158/1538-7445.SABCS18-P5-04-18

33. Qi S-M, Dong J, Xu Z-Y, Cheng X-D, Zhang W-D, Qin J-J (2021) PROTAC: An Effective Targeted Protein Degradation Strategy for Cancer Therapy. Frontiers in Pharmacology 12

34. Tae HS, Sundberg TB, Neklesa TK, Noblin DJ, Gustafson JL, Roth AG, Raina K, Crews CM (2012) Identification of hydrophobic tags for the degradation of stabilized proteins. Chembiochem 13 (4):538-541. doi:10.1002/cbic.201100793

35. Neklesa TK, Tae HS, Schneekloth AR, Stulberg MJ, Corson TW, Sundberg TB, Raina K, Holley SA, Crews CM (2011) Small-molecule hydrophobic tagging–induced degradation of HaloTag fusion proteins. Nature Chemical Biology 7 (8):538-543. doi:10.1038/nchembio.597

36. Long Marcus JC, Gollapalli Deviprasad R, Hedstrom L (2012) Inhibitor Mediated Protein Degradation. Chemistry & Biology 19 (5):629-637. doi:https://doi.org/10.1016/j.chembiol.2012.04.008

37. Collins I, Wang H, Caldwell JJ, Chopra R (2017) Chemical approaches to targeted protein degradation through modulation of the ubiquitin-proteasome pathway. Biochem J 474 (7):1127-1147. doi:10.1042/bcj20160762

38. Neklesa TK, Noblin DJ, Kuzin A, Lew S, Seetharaman J, Acton TB, Kornhaber G, Xiao R, Montelione GT, Tong L, Crews CM (2013) A Bidirectional System for the Dynamic Small Molecule Control of Intracellular Fusion Proteins. ACS Chemical Biology 8 (10):2293-2300. doi:10.1021/cb400569k

39. Shi Y, Long MJC, Rosenberg MM, Li S, Kobjack A, Lessans P, Coffey RT, Hedstrom L (2016) Boc3Arg-Linked Ligands Induce Degradation by Localizing Target Proteins to the 20S Proteasome. ACS Chemical Biology 11 (12):3328-3337. doi:10.1021/acschembio.6b00656

40. Gustafson JL, Neklesa TK, Cox CS, Roth AG, Buckley DL, Tae HS, Sundberg TB, Stagg DB, Hines J, McDonnell DP, Norris JD, Crews CM (2015) Small-Molecule-Mediated Degradation of the Androgen Receptor through Hydrophobic Tagging. Angewandte Chemie International Edition 54 (33):9659-9662. doi:https://doi.org/10.1002/anie.201503720

41. Ma A, Stratikopoulos E, Park K-S, Wei J, Martin TC, Yang X, Schwarz M, Leshchenko V, Rialdi A, Dale B, Lagana A, Guccione E, Parekh S, Parsons R, Jin J (2020) Discovery of a first-in-class EZH2 selective degrader. Nature Chemical Biology 16 (2):214-222. doi:10.1038/s41589-019-0421-4

42. Xie T, Lim SM, Westover KD, Dodge ME, Ercan D, Ficarro SB, Udayakumar D, Gurbani D, Tae HS, Riddle SM, Sim T, Marto JA, Jänne PA, Crews CM, Gray NS (2014) Pharmacological targeting of the pseudokinase Her3. Nat Chem Biol 10 (12):1006-1012. doi:10.1038/nchembio.1658

43. Qiu J, Bai X, Zhang W, Ma M, Wang W, Liang Y, Wang H, Tian J, Yu P (2022) LPM3770277, a Potent Novel CDK4/6 Degrader, Exerts Antitumor Effect Against Triple-Negative Breast Cancer. Frontiers in Pharmacology 13

44. Choi SR, Wang HM, Shin MH, Lim H-S (2021) Hydrophobic Tagging-Mediated Degradation of Transcription Coactivator SRC-1. International Journal of Molecular Sciences 22 (12). doi:10.3390/ijms22126407

45. Long X, Nephew KP (2006) Fulvestrant (ICI 182,780)-dependent Interacting Proteins Mediate Immobilization and Degradation of Estrogen Receptor-α*. J Biol Chem 281 (14):9607-9615. doi:https://doi.org/10.1074/jbc.M510809200

46. Yang K, Song Y, Xie H, Wu H, Wu Y-T, Leisten ED, Tang W (2018) Development of the first small molecule histone deacetylase 6 (HDAC6) degraders. Bioorg Med Chem Lett 28 (14):2493-2497. doi:https://doi.org/10.1016/j.bmcl.2018.05.057

47. Liu J-R, Yu C-W, Hung P-Y, Hsin L-W, Chern J-W (2019) High-selective HDAC6 inhibitor promotes HDAC6 degradation following autophagy modulation and enhanced antitumor immunity in glioblastoma. Biochem Pharmacol 163:458-471. doi:https://doi.org/10.1016/j.bcp.2019.03.023

48. Yang K, Wu H, Zhang Z, Leisten ED, Nie X, Liu B, Wen Z, Zhang J, Cunningham MD, Tang W (2020) Development of Selective Histone Deacetylase 6 (HDAC6) Degraders Recruiting Von Hippel–Lindau (VHL) E3 Ubiquitin Ligase. ACS Med Chem Lett 11 (4):575-581. doi:10.1021/acsmedchemlett.0c00046

49. Wu H, Yang K, Zhang Z, Leisten ED, Li Z, Xie H, Liu J, Smith KA, Novakova Z, Barinka C, Tang W (2019) Development of Multifunctional Histone Deacetylase 6 Degraders with Potent Antimyeloma Activity. J Med Chem 62 (15):7042-7057. doi:10.1021/acs.jmedchem.9b00516

50. Xiao Y, Wang J, Zhao LY, Chen X, Zheng G, Zhang X, Liao D (2020) Discovery of histone deacetylase 3 (HDAC3)-specific PROTACs. Chem Commun 56 (68):9866-9869. doi:10.1039/D0CC03243C

51. Chotitumnavee J, Yamashita Y, Takahashi Y, Takada Y, Iida T, Oba M, Itoh Y, Suzuki T (2022) Selective degradation of histone deacetylase 8 mediated by a proteolysis targeting chimera (PROTAC). Chemical Communications 58 (29):4635-4638. doi:10.1039/D2CC00272H

52. Heimburg T, Chakrabarti A, Lancelot J, Marek M, Melesina J, Hauser A-T, Shaik TB, Duclaud S, Robaa D, Erdmann F, Schmidt M, Romier C, Pierce RJ, Jung M, Sippl W (2016) Structure-Based Design and Synthesis of Novel Inhibitors Targeting HDAC8 from Schistosoma mansoni for the Treatment of Schistosomiasis. Journal of Medicinal Chemistry 59 (6):2423-2435. doi:10.1021/acs.jmedchem.5b01478

53. Marek M, Shaik TB, Heimburg T, Chakrabarti A, Lancelot J, Ramos-Morales E, Da Veiga C, Kalinin D, Melesina J, Robaa D, Schmidtkunz K, Suzuki T, Holl R, Ennifar E, Pierce RJ, Jung M, Sippl W, Romier C (2018) Characterization of Histone Deacetylase 8 (HDAC8) Selective Inhibition Reveals Specific Active Site Structural and Functional Determinants. J Med Chem 61 (22):10000-10016. doi:10.1021/acs.jmedchem.8b01087

54. Lai AC, Toure M, Hellerschmied D, Salami J, Jaime-Figueroa S, Ko E, Hines J, Crews CM (2016) Modular PROTAC Design for the Degradation of Oncogenic BCR-ABL. Angew Chem Int Ed 55 (2):807-810. doi:https://doi.org/10.1002/anie.201507634

55. Smith BE, Wang SL, Jaime-Figueroa S, Harbin A, Wang J, Hamman BD, Crews CM (2019) Differential PROTAC substrate specificity dictated by orientation of recruited E3 ligase. Nat Commun 10 (1):131. doi:10.1038/s41467-018-08027-7

56. Cyrus K, Wehenkel M, Choi EY, Han HJ, Lee H, Swanson H, Kim KB (2011) Impact of linker length on the activity of PROTACs. Mol Biosyst 7 (2):359-364. doi:10.1039/c0mb00074d

57. Zorba A, Nguyen C, Xu Y, Starr J, Borzilleri K, Smith J, Zhu H, Farley KA, Ding W, Schiemer J, Feng X, Chang JS, Uccello DP, Young JA, Garcia-Irrizary CN, Czabaniuk L, Schuff B, Oliver R, Montgomery J, Hayward MM, Coe J, Chen J, Niosi M, Luthra S, Shah JC, El-Kattan A, Qiu X, West GM, Noe MC, Shanmugasundaram V, Gilbert AM, Brown MF, Calabrese MF (2018) Delineating the role of cooperativity in the design of potent PROTACs for BTK. Proc Natl Acad Sci U S A 115 (31):E7285-e7292. doi:10.1073/pnas.1803662115

58. Nowak RP, DeAngelo SL, Buckley D, He Z, Donovan KA, An J, Safaee N, Jedrychowski MP, Ponthier CM, Ishoey M, Zhang T, Mancias JD, Gray NS, Bradner JE, Fischer ES (2018) Plasticity in binding confers selectivity in ligand-induced protein degradation. Nat Chem Biol 14 (7):706-714. doi:10.1038/s41589-018-0055-y

59. Cyrus K, Wehenkel M, Choi E-Y, Lee H, Swanson H, Kim K-B (2010) Jostling for Position: Optimizing Linker Location in the Design of Estrogen Receptor-Targeting PROTACs. ChemMedChem 5 (7):979-985. doi:https://doi.org/10.1002/cmdc.201000146

60. Zoppi V, Hughes SJ, Maniaci C, Testa A, Gmaschitz T, Wieshofer C, Koegl M, Riching KM, Daniels DL, Spallarossa A, Ciulli A (2019) Iterative Design and Optimization of Initially Inactive Proteolysis Targeting Chimeras (PROTACs) Identify VZ185 as a Potent, Fast, and Selective von Hippel–Lindau (VHL) Based Dual Degrader Probe of BRD9 and BRD7. J Med Chem 62 (2):699-726. doi:10.1021/acs.jmedchem.8b01413

61. Darwish S, Heimburg T, Ridinger J, Herp D, Schmidt M, Romier C, Jung M, Oehme I, Sippl W (in press) Synthesis, Biochemical and Cellular Evaluation of HDAC6 targeting proteolysis targeting chimeras. In. Methods in Molecular Biology, HDAC/HAT Function Assessment and Inhibitor Development: Methods and Protocols, Second Edition edn. Springer Nature,

62. Ghazy E, Zeyen P, Herp D, Hügle M, Schmidtkunz K, Erdmann F, Robaa D, Schmidt M, Morales ER, Romier C, Günther S, Jung M, Sippl W (2020) Design, synthesis, and biological evaluation of dual targeting inhibitors of histone deacetylase 6/8 and bromodomain BRPF1. Eur J Med Chem 200:112338. doi:https://doi.org/10.1016/j.ejmech.2020.112338

63. Stolfa DA, Stefanachi A, Gajer JM, Nebbioso A, Altucci L, Cellamare S, Jung M, Carotti A (2012) Design, Synthesis, and Biological Evaluation of 2-Aminobenzanilide Derivatives as Potent and Selective HDAC Inhibitors. ChemMedChem 7 (7):1256-1266. doi:https://doi.org/10.1002/cmdc.201200193

64. Marek M, Kannan S, Hauser A-T, Moraes Mourão M, Caby S, Cura V, Stolfa DA, Schmidtkunz K, Lancelot J, Andrade L, Renaud J-P, Oliveira G, Sippl W, Jung M, Cavarelli J, Pierce RJ, Romier C (2013)

Structural Basis for the Inhibition of Histone Deacetylase 8 (HDAC8), a Key Epigenetic Player in the Blood Fluke Schistosoma mansoni. PLOS Pathogens 9 (9):e1003645. doi:10.1371/journal.ppat.1003645

65. Samadi S, Jadidi K, Khanmohammadi B, Tavakoli N (2016) Heterogenization of chiral mono oxazoline ligands by grafting onto mesoporous silica MCM-41 and their application in copper-catalyzed asymmetric allylic oxidation of cyclic olefins. J Catal 340:344-353. doi:https://doi.org/10.1016/j.jcat.2016.05.021

66. Nagaoka Y, Maeda T, Kawai Y, Nakashima D, Oikawa T, Shimoke K, Ikeuchi T, Kuwajima H, Uesato S (2006) Synthesis and cancer antiproliferative activity of new histone deacetylase inhibitors: hydrophilic hydroxamates and 2-aminobenzamide-containing derivatives. Eur J Med Chem 41 (6):697-708. doi:https://doi.org/10.1016/j.ejmech.2006.02.002

67. Tang W, Luo T, Greenberg EF, Bradner JE, Schreiber SL (2011) Discovery of histone deacetylase 8 selective inhibitors. Bioorganic & Medicinal Chemistry Letters 21 (9):2601-2605. doi:https://doi.org/10.1016/j.bmcl.2011.01.134

68. Kubik S, Goddard R (2001) Fine tuning of the cation affinity of artificial receptors based on cyclic peptides by intramolecular conformational control. European Journal of Organic Chemistry 2001 (2):311-322. doi:10.1002/1099-0690(200101)2001:2<311::Aid-ejoc311>3.0.Co;2-m